Rational Design and Preliminary Validation of Novel

6-Phosphogluconate Dehydrogenase (6PGD) Inhibitors Using

Parietin as a Lead

Submitted in partial fulfilment of the requirements of the Degree of Master of

Pharmacy

Daniel Sinagra

Department of Pharmacy

2021

Abstract

Parietin has documented anti-tumour properties through inhibition of the 6-phosphogluconate dehydrogenase (6PGD) enzyme which is involved in tumour cell metabolism as part of the overactive pentose phosphate pathway (PPP). In this study, the parietin molecule was used as a scaffold for the design and identification of new molecules capable of similar modulation of the 6PGD enzyme using both virtual screening and de novo design.

The study was guided by crystallographic deposition 2IZ1 which describes small molecule inhibitor PEX bound to 6PGD. PEX was extracted from 2IZ1 and the parietin structure was modelled in SYBYL®-X. Using the parietin structure as a general pharmacophore, 4 hit molecules were identified using virtual screening from the online ZINC Pharmer database®. The next phase of the study involved the identification of the optimal conformer of parietin inside the 6PGD ligand binding pocket. The optimal conformer identified through this study was used as the basis for the de novo approach. A 2D topology map describing the interactions of the optimal conformer of parietin with the 6PGD ligand binding pocket was generated, and 3 seed molecules were subsequently modelled keeping the moieties essential for binding. These seed structures were inputted in LigBuilder v1.2 where the molecules were allowed to grow within the crystallographically described 6PGD ligand binding pocket. A series of molecules was consequently generated. The highest affinity Lipinski Rule compliant structure was compared with its lowest affinity counterparts from an atomic perspective based on the creation of 2D topology maps which described their critical interactions with the target receptor. A similar comparison was also carried out between the highest

affinity de novo designed molecules and the lead molecule parietin. This allowed identification of the conserved amino acids critical to 6PGD modulation. These include the amino acids Ala^{12}, Arg^{34}, Asn^{33} and Val^{74}.

Table of Contents

List of Tables

List of Figures

List of Abbreviations

6PGD: 6-Phosphogluconate Dehydrogenase

PPP: Pentose Phosphate Pathway

G6P: Glucose-6-Phosphate

F6P: Fructose-6-Phosphate

G3P: Glyceraldehyde-6-phosphate

NADPH: Nicotinamide adenine dinucleotide phosphate

JAK2: Janus kinase 2

STAT3: Signal transducer and activator of transcription 3

Atg5: Autophagy related 5

MMP: Matrix metalloproteinase

R5P: Ribose-5-phosphate

G6PD: Glucose-6-phosphate dehydrogenase

6PG: 6-phoshpogluconate

Ru5P: Ribulose-5-phosphate

ROS: Reactive oxygen species

$NADP^+$: A reduced form of $NADP^+$

LKB1: Liver kinase B1

AMPK: Adenine monophosphate-activated protein kinase

STRAD: Ste20-related adaptor

MO25: Mouse protein 25

ACC: Acetyl CoA carboxylase

RhoA: Ras homolog gene family, member A

Rac1: Ras-related C3 botulinum toxin substrate 1

Ll6PGD: 6PGD from *Lactococcus lactis*

OaPDH: 6PGD from *Ovis aries*

CO_2: Carbon Dioxide

6PGL: 6-Phosphogluconolactone

GL: Gluconolactonase

6ANAD: 6-Aminonicotinamide adenine dinucleotide

PEX: 4-Phospho-D-erythronohydroxamic acid

PEA: 4-Phospho-D-erythonamide

6AN: 6-Aminonicotinamide

DMSO: Dimethyl sulfoxide

VS: Virtual Screening

SAR: Structure activity relationship

Chapter 1

Literature Review

1.1 Introduction

Malignant disease is one of the most common causes of mortality and has accounted for 9.6 million deaths globally as of 2018[1]. Many risk factors associated with cancers have been identified up to date including smoking, obesity, diet, and physical inactivity. Lung cancer in males and breast cancer in females are the most frequently diagnosed cancers and the most common cause of cancer mortality globally (Bray *et al.* 2018). Apart from these, other cancers such as prostate cancer in males, uterine and ovarian cancers in females and colon and rectal cancers in both males and females are also a cause of cancer associated deaths. Current cancer treatment includes surgery, radio therapy, chemotherapy, immunotherapy, hormone therapy and stem cell transplantation.[1]

1.2 The Role of 6-Phosphogluconate Dehydrogenase in Carcinogenesis

6-phosphogluonate dehydrogenase (6PGD) is the third enzyme in the pentose pathway (PPP) [Figure 1.1]. The PPP is an important pathway in cancer cell proliferation and growth and is seen to have an increased activity in certain types of cancer cells (Richardson *et al.*, 2008). The PPP can be thought of as a shunt to normal glycolysis, as glucose-6-phosphate (G6P), the second product of glycolysis participates as the first substrate in the PPP. Ultimately, fructose-6-phosphate (F6P) and glyceraldehyde-6-phosphate (G3P), which are products produced in

---

[1] World Health Organisation [Internet]. Cancer. 2018. Available from: http://www.who.int/cancer/en/. [cited 23.04.2018]
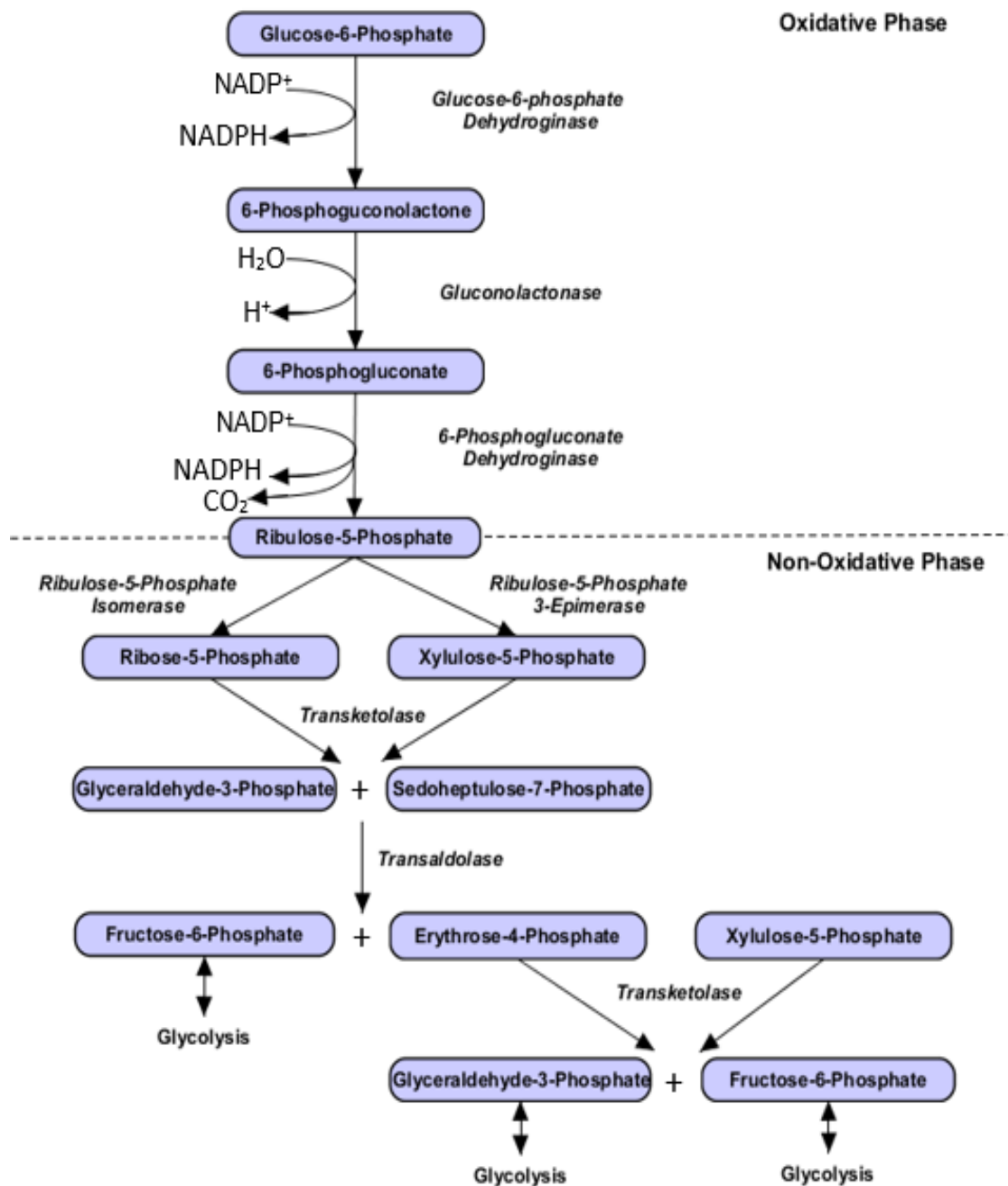
Figure 1.1 The PPP showing both the oxidative phase and the non-oxidative phase. G6P enters from glycolysis while G3P produced by the PPP is able to participate in glycolysis. F6P is able to enter the PPP from glycolysis as well as exit the PPP to participate in glycolysis. This pathway was rendered using PathVisio®.[2]

---

[2] Available from: https://www.pathvisio.org/downloads/

the non-oxidative phase of the PPP are directly supplied to continue their use in glycolysis. The oxidative phase of the PPP uses G6P from oxidative phosphorylation to produce mainly two important products which are the reduced form of nicotinamide adenine dinucleotide phosphate (NADPH), a reducing agent which protects the cell from oxidative stress, and ribose-5-phosphate (R5P), a precursor of nucleotide synthesis. NADPH production is mediated by two enzymes in this pathway, namely; glucose-6-phosphate dehydrogenase (G6PD), which is the first enzyme in the PPP, and 6PGD. 6PGD turns 6-phoshpogluconate (6PG) into ribulose-5-phosphate (Ru5P) producing NADPH and CO_2 as by-products (Lehinger *et al.,* 2000; Wood, 1986).

The PPP is known to operate in tissues which are exposed to a high degree of oxidative stress and in those which undergo constant cell division (Pandolfi *et al.,* 1995). This explains the over-expression of this pathway in proliferating tumour tissues. It has already been established that a high degree of reactive oxygen species (ROS) are produced in cellular detachment as seen in cancer metastasis (Schafer *et al.,* 2009) and that cancer cells use the PPP product NADPH to combat such oxidative stress (Cairns *et al.,* 2011). Cancer cells can evade anoikis and H_2O_2 mediated apoptosis, which produce high levels of ROS, proving the importance of the PPP for tumour survival (Frisch & Francis, 1994).

It appears that the cause of growth and proliferation in cancer cells is not directly linked to the inhibition of the PPP, but rather through the inhibition of 6PGD alone (Lin *et al.*, 2015). 6PGD is found to be overexpressed in cancer cells by lysine acetylation at two specific regions of the enzyme. These regions include; K76, where binding of nicotinamide adenine dinucleotide phosphate (NADP+) to 6PGD is promoted, and K294,

an area which promotes the dimerization of monomeric 6PGD, resulting in a homodimer enzyme. This acetylation process serves as an important mechanism for the growth and proliferation of the tumour (Shan *et al.*, 2014).

6PGD is found to play an active role in controlling the levels of RNA and DNA biosynthesis of the cell as well as maintaining redox homeostasis with the production of Ru5P and NADPH respectively. In 2015, Lin *et al.* found that Ru5P can inhibit liver kinase B1 (LKB1), a tumour suppressor which serves as an upstream kinase of adenine monophosphate-activated protein kinase (AMPK). AMPK has the potential of stopping lipogenesis, the production of fatty acid and cholesterol, components which are in demand during cell division. LKB1 produces a complex with pseudokinase Ste20-related adaptor (STRAD) and scaffolding-like adaptor protein mouse protein 25 (MO25) to produce an LKB1-MO25-STRAD complex. This complex activates AMPK, initiating LKB1-AMPK signalling which is capable of phosphorylating acetyl CoA carboxylase (ACC) enzymes 1 and 2, causing their inhibition and in turn decrease the ability of the tumour cells to handle oxidative stress and carry out lipogenesis. AMPK activation has also been associated with decreased cell migration by the decreased activity of RhoA and Rac1 proteins in cervical cancer cells (Guo *et al.,* 2018).

Therefore, lack of 6PGD either by inhibition or knockdown would result in a decreased amount of NADPH and Ru5P, making the tumour cell less able to handle oxidative stress and to initiate lipogenesis. These findings where not observed in normal proliferating cells of the keratinocyte HaCaT type, suggesting that normal cells do not extensively rely on the production of Ru5P for lipogenesis and maintenance of redox homeostasis. This gives a reason to believe that 6PGD can serve as an important target for cancer

treatment in the way that it controls tumour growth and proliferation as well as its abundance in tumour cells.

1.3 The Structure of 6-Phosphogluconate Dehydrogenase

In 2007, Sundaramoorthy *et al.,* published a study using 6PGD from *Lactococcus lactis* (L*l*6PGD) [Figure 1.2i] as it shares 58% of its amino acid sequence with the mammalian 6PGD enzyme from sheep (O*a*PDH), which is commonly extracted from their liver (Silverberg and Dalziel *et al.,* 1973; Adams *et al.,* 1983). L*l*6PGD, like other 6PGD enzymes has subunits [Figure 1.2ii] of a molecular weight of 52kDa and are made up of 472 amino acids [Figure 1.2iii] with 10 β strands and 21 α helices. 6PGD is an asymmetric homodimer enzyme composed of three subunits, two of which (subunits A and B) form a symmetric dimer, and a monomer (subunit C) joining them together. The subunits of 6PGD compromise of three domains; domains I (residues 1-177), II (residues 178-433) and III (residues 434-468). Domain II is the longest domain compromising of 256 residues, while domain 3 is the shortest compromising of 35 residues. Therefore, the 6PGD enzyme is able to bind two $NADP^+$ molecules and two 6PG molecules. In 1983, Adams *et al.,* described O*a*PDH as being made up of 2 domains rather than 3 as described by Sundaramoorthy *et al.* These domains include the larger domain

constituting of residues 33-344 and 438-466, and the smaller domain constituting of residues 345-437.
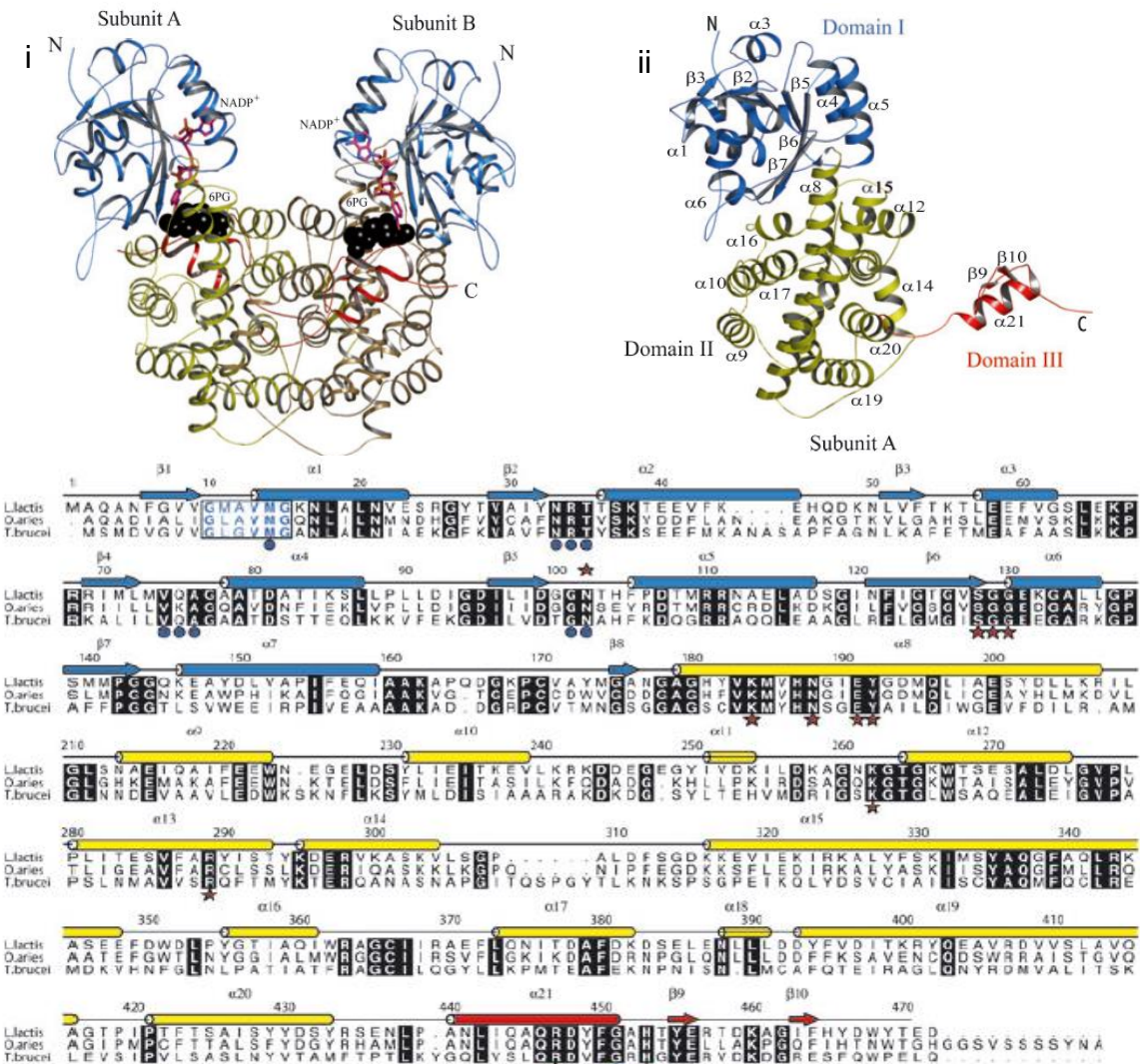
Figure 1.2 (i) The ribbon diagram of one of the subunits of L*l*6PGD. Blue ribbons indicate Domain I, yellow ribbons indicate domain II and red ribbons indicate domain III. **(ii)** The *holo* form of the L*l*6PGD homodimer showing two bound 6PG molecules as black spheres and two bound NADP+ molecules as stick models. **(iii)** A description of the amino acid sequence and secondary protein structure of L*l*6PGD. β strands (β1-β10) are shown as arrows while α helices (α1-α21) are shown as cylinders. Blue structures make-up domain I, yellow structures make-up domain II while red structures make-up domain III. Adopted from: Sundaramoorthy R, Iulek J, Barret MP, Bidet O, Ruda GF, Gilbert IH *et al.* Crystal structures of a bacterial 6-phosphogluconate dehydrogenase reveal aspects of specificity, mechanism

and mode of inhibition by analogues of high-energy reaction intermediates. FEBS J. 2007;274(1):275-276.

1.3.1 The cofactor binding site

Domain I of 6PGD contains the binding site for the cofactor NADP+. Ala12 limits the capacity for NADP+ to bind into its pocket due to its protrusion into the ligand binding pocket. The adenine group of NADP+ is held against Arg34, an important amino acid for the binding of this cofactor with 6PGD (Tetaud et al., 1999), and forms hydrophobic interactions with Ala78 and Ala79. In OaPDH, Arg33 was found to be responsible for the specificity of OaPDH to NADP+ (Adams et al., 1994). In Ll6PGD the 2'-phosphate shares hydrogen bonds with amino acids Asn33, Arg34 and Thr35, causing the main chain of the α2 helix to move by about 1 Å. The ribose hydroxyl and phosphate groups form hydrogen bonds with Gln75 and Asn13. Met14 is recognised as important in the positioning of the nicotinamide group of the cofactor as it forms hydrogen bonds with the pyrophosphate group, causing a change in side-chain orientation. The nicotinamide ribose part is held by hydrogen bonds with Val74, Asn102 and Ala76. The carbonyl from the nicotinamide group can form a hydrogen bond with either the C4-hydroxyl of 6PG substrate or the C3-hydroxyl of Ru5P product (Sundaramoorthy et al., 2007).

1.3.2 The catalytic site

The active site for 6PG is a pocket made up by residues from the three domains with α8 serving as the base. The C1 of 6PG is near to the binding site of NADP+ with the phosphate group pointing to the loop between α10-α11 and domain III of the other subunit. This phosphate group is stabilised by hydrogen bonds formed with Tyr191, Arg287, Arg447 and Lys262, where the latter covers the active site after phosphate binding. Water molecules play a role in mediating hydrogen bonds between the enzyme

and the substrate. A water molecule mediates the interactions between the phosphate group of 6PG and Gly263 and Thr264 while 4-OH interacts with His453 and another water molecule. C4 of 6PG cannot exist in an R-conformation when bound as this would lead to a steric collision with Asn102, in which the latter is bonded via a hydrogen bond with C3-OH (Sundaramoorthy et al., 2007).

Hanau et al., (2010) proposed that 6PGD subunits have the potential to influence one another. For the conversion of 6PG to Ru5P, NADPH needs to be formed already, however it does not participate in the conversion of 6PG to Ru5P as a redox partner. Sundaramoorthy et al. suggested that the NADP+ binding domain moves in such a way to allow cooperative binding of 6PG. They also proposed a model of the two subunits carrying out different reactions, one subunit carries out decarboxylation of 6PG while the other oxidises 6PG, finally switching their roles repeating the process. (Hanau et al., 2010; Sundaramoorthy et al., 2007).

1.4 Endogenous agonists of 6-Phosphogluconate Dehydrogenase

1.4.1 The cofactor

NADP+ [Figure 1.3i] is a coenzyme which serves its role in many anabolic reactions such as in the synthesis of lipids and nucleic acids. This cofactor serves as an electron carrier and thus it is reduced to NADPH. It has the chemical formula $C_{21}H_{29}N_7O_{17}P_3^+$ and has a molecular weight of 744.416 g/mol. The cofactor has 9 hydrogen bond donors, 21 hydrogen bond acceptors and 13 rotatable bonds.[3] The structure of NADP$^+$ compromises

---

[3] PubChem Compound Database [Internet]. Available from:
https://pubchem.ncbi.nlm.nih.gov/compound/nadp_ [cited 28.04.2018]

of ribosylnicotinamide 5-phosphate linked to 5-phosphate adenosine 2, 5-bisphosphate by a pyrophosphate linkage.

1.4.2 The Substrate

6PG [Figure 1.3ii] is a monosaccharide phosphate and serves as the substrate of 6PGD which undergoes oxidative decarboxylation to Ru5P and carbon dioxide (CO_2). It is formed by hydrolysis of 6-Phosphogluconolactone (6PGL) by the enzyme gluconolactonase (GL). 6PG has a chemical formula $C_6H_{13}O_{10}P$ and a molecular weight of 276.134 g/mol. The molecule has 7 hydrogen bond donors, 10 hydrogen bond acceptors and 7 rotatable bonds.[4] C1 contains a carboxyl group, C2 until C5 contain a hydroxyl group while C6 binds a phosphate group.
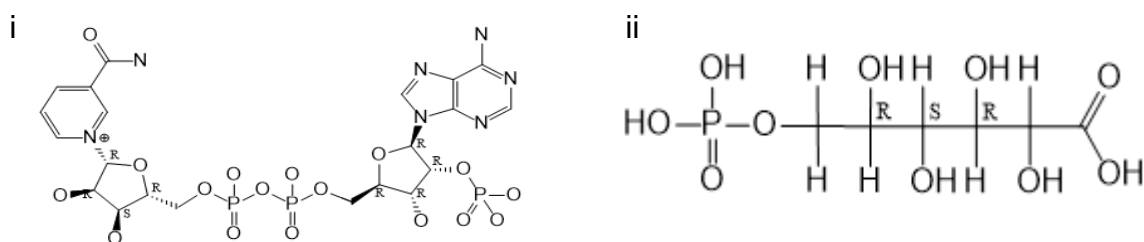
Figure 1.3 The two-dimensional structures of **(i)** the cofactor NADP^{+}. **(ii)** the substrate 6PG. Both structures where rendered using KnowItAll® Academic Edition.[5]

1.5 Antagonists of 6-Phosphogluconate Dehydrogenase

Molecules that are known to inhibit the activity of 6PGD include 6-aminonicotinamide adenine dinucleotide (6ANAD) (Lange and Proft, 1970), 4-phospho-D-

[4] PubChem Compound Database [Internet]. Available from:
https://pubchem.ncbi.nlm.nih.gov/compound/6-phosphogluconic_acid [cited 28.04.2018]
[5] Bio-Rad: KnowItAll® Academic Edition. Version 18.0.53 [software]. Available from:
https://www.biorad.com/en-mt/product/knowitall-academic-edition-free-chemistry-software?ID=NH29WJ15.

erythronohydroxamic acid (PEX) and 4-phospho-D-erythonamide (PEA) (Sundaramoorthy et al., 2007), parietin (or physcion) and its semi-synthetic derivative S3 (Lin *et al.*, 2015). 6ANAD inhibits 6PGD by inhibiting the binding of the cofactor $NADP^+$ with its active site. This was shown by Lange and Proft in 1970 by administering 6-aminonicotinamide (6AN) to mice. 6AN was converted to 6ANAD by the NAD-glycohydrolase enzyme in mouse liver and kidney. 6AN is considered toxic (Johnson and McColl, 1955) and thus has no use in the treatment of neoplastic disease.

PEX [Figure 1.4i] and PEA [Figure 1.4ii], which have similar structures, bind to 6PGD in a similar fashion as 6PG and Ru5P. Both inhibitors differ in functional groups attached to C1, where PEX contains a hydroxamate group while PEA contains an acid amide group. Phosphate groups interact with Tyr^{192}, Arg^{289} and Arg^{447} while functional groups of PEX and PEA bond with the enzyme via hydrogen bonding. Both interact with $NADP^+$ where C2-OH accepts a hydrogen bond from His^{435} of the other subunit and donates a bond to the nicotinamide carbonyl. A water molecule mediates the interaction occurs between the C3-OH of PEX/PEA and the nicotinamide ribose. The amide group of PEX and PEA links and the amide group of Gly^{130} by a water molecule as well. Having a hydroxyl group, PEX donates a hydrogen bond from the hydroxamate group to the catalytic Glu191 while PEA, which lacks a hydroxyl group on N1 , interacts with Glu^{191} via a water mediated link. The extra hydroxyl group in PEX results in a stronger inhibition of 6PGD than PEA, thus proving the importance of the extra group. Up until now, there are no studies which deal with the effects of either PEX or PEA on cancer cells and the human body (Sundaramoorthy et al., 2007).

Parietin [Figure 1.4iii] and its derivative S3 [Figure 1.4iv], have a common anthraquinone base, however they differ in the number of functional groups and their position. Lin *et al., (2015)* suggested that parietin docks at a pocket near the binding site of 6PG, forming hydrophobic interactions with Met[15], Lys[76], Lys[261] and His[452] of 6PGD. Furthermore, the 10-keto group of parietin links to Asn[103] through a hydrogen bond. Various studies show the anti-tumour (Lin *et al.,* 2015; Bačkorová *et al.,* 2011), anti-metastatic (Yan-Tao *et al.,* 2015) and pro-apoptotic (Chen *et al.,* 2015; Elf *et al.,* 2017; Pan *et al.,* 2018a) effects of parietin.
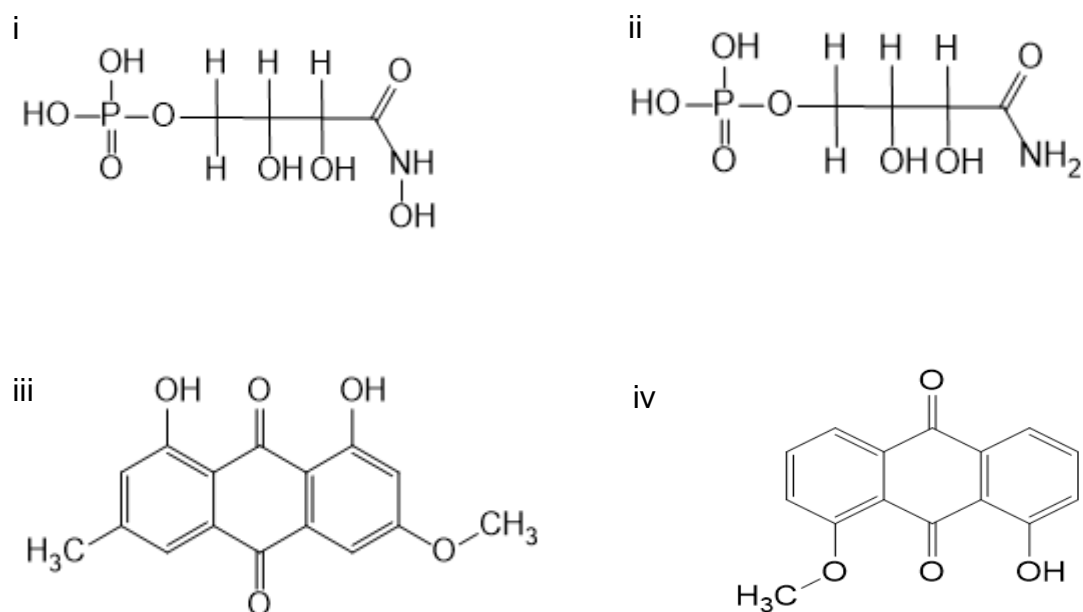

Figure 1.4 The two-dimensional structures of **(i)** PEX **(ii)** PEA **(iii)** Parietin **(iv)** S3. All four structures where rendered using KnowItAll® Academic Edition.[5]

In 2015, Lin *et al.* conducted a study on the effects of both parietin and S3 on cancer cells by the inhibition of 6PGD. They found that parietin reduced the 6PGD product Ru5P and increased the substrate concentration of 6PG of human cancer cell lines *in vitro*. Parietin however also decreased the activity of 6PGD in normal proliferating HaCaT cells, however their proliferation rate was not affected. They also sought to evaluate the effects of S3 on nude mice and found that administration of 20 mgkg^{-1} of S3 by intraperitoneal injections for about four weeks resulted in a dosage that was well-tolerated. Furthermore, treatment with S3 on nude mice which have been previously injected with H1299 cells subcutaneously showed a noteworthy decrease in tumour growth and tumour mass compared to the nude mice receiving the control treatment of dimethyl sulfoxide (DMSO). Another xenograft using K562 leukaemia cells on nude mice also achieved similar results. Most importantly, chronic S3 treatment did not alter physical and physiological parameters of nude mice compared to those treated with DMSO (Lin *et al.,* 2015). In another study done by Pan *et al. (2018b)*, 40 mgkg^{-1}day^{-1} of parietin administered to mice did not show any signs of damage in healthy tissues of mice. A Phase I clinical study carried out by Tsang-Bin *et al*., (2010) concluded that ingestion of up to 250mg of parietin each day for the duration of 14 days produced no significant adverse effects and is well tolerated.

Parietin has been shown to increase the effectiveness of certain chemotherapeutic drugs such as paclitaxel and cisplatin due to inhibition of 6PGD (Chen *et al.,* 2019; Guo *et al.,* 2018). Guo *et al.* found that cervical cancer cells treated with both parietin and paclitaxel resulted in inhibition of proliferation, increased apoptosis and an 80-90% inhibition of growth and survival of the cancer cells than if treated with paclitaxel alone. Another study carried out by Liu *et al.* (2016) suggests that parietin causes upregulation

of miR-146a reversing adriamycin resistance of the adriamycin resistant chronic myelogenous leukaemia cells K562. This indicates that parietin may be used concurrently with such drugs to reach the desired therapeutic effect with decreased side effects associated with such chemotherapeutic agents.

These findings prove the effectiveness of S3 *in vivo*. Thus, parietin and its semi-synthetic derivative S3 prove to be promising molecules in the treatment of neoplastic disease.

1.6 Parietin

Parietin or physcion, whose structure is shown in Figure 1.4 (iii), is an orange coloured anthraquinone pigment found mainly in the lichen *Xanthoria parietina* as well as in the fungus *Microsporium* sp and in rhubarb, has been shown to have medicinal potential as an antibacterial, antifungal as well as anticancer agent (Basile *et al.,* 2009). In 2015, Lin *et al*. chose parietin and its semi-synthetic derivative S3 as molecules which inhibit the NADP$^+$ dependent 6PGD, but do not inhibit other NADP$^+$ dependent enzymes including G6PD, glutamate dehydrogenase 1, isocitrate dehydrogenase and neither glycolytic enzymes lactate dehydrogenase A and phosphoglycerate mutase 1. Qin *et al.* (2018) identified the anthraquinone emodin as a metabolite of parietin. Emodin has been reported to cause nephrotoxicity (Li *et al.*, 2010) and hepatotoxicity (Li *et al.*, 2012). These findings show that parietin along with S3 have selectivity for 6PGD, an important quality for the targeting of this enzyme in cancer treatment (Lin *et al.,* 2015).

1.7 Rational Drug Design

In the search for better drugs for the treatment of diseases, we moved away from less specific methods of drug discovery which included tradition and serendipity to more specific methods of rational drug design. Rational drug design involves the use of

modern technology to aid and speed the process of drug discovery. Methods of such drug discovery include high throughput screening and virtual screening (VS) for targets whose functions and structures we know by X-Ray crystallography. This method involves the use of finding the candidate molecules which have potential to fit in the target. Another means of modern drug discovery is biological screening which can be used for potent drugs, whose targets we do not know (Mandal *et al.,* 2009).

1.7.1 BIOVA Discovery Studio Visualizer® v17.2

BIOVA Discovery Studio Visualizer®[6] is a software that allows users to view *pdb* and *mol2* file formats in 3D renditions. This program allows for in silico simulation of ligand-receptor interactions and gives necessary information on current observations and for further development.

1.7.2 SYBYL®-X v1.1

SYBYL®-X (Ash *et al*., 2010) is a software which allows for the design and optimisation of lead molecules. This program gives information on structure activity relationship (SAR) and the pharmacophores. Knowing the SAR properties, SYBYL®-X can predict pharmacokinetic and physical properties of the molecules.

---

[6] Dassault Systèmes. BIOVIA Discovery Studio Visualizer. Version 20.1 [software]. Dassault Systèmes. 2020 [cited 2021 Jul 14; downloaded 2021 May 25]. Available from: https://www.3dsbiovia.com/products/collaborative-science/biovia-discovery-studio/visualization-download.php.

1.7.3 KnowItAll® Academic Edition v18

KnowItAll®Academic Edition[5] is a free software which provides interfaces for the drawing of chemical structures and reporting and publishing tools (ChemWindow), and tools for spectral analysis.

1.7.4 X-Score® v1.2

X-Score® (Wang et al., 2002) is a program which can compute the binding affinities of the ligand molecule in question to its designated protein, thus it is called a 'scoring function'.

1.7.5 UCSF Chimera® v1.12

Chimera® (Petterson *et al.,* 2004) is a free software which allows for the visualisation and analysis of molecular structures. It allows for density mapping of the structure as well as supramolecular assemblies, alignment of sequences, docking and trajectories and viewing of the different structural conformations of the molecule.

1.7.6 ZINCPharmer®

ZINCPharmer® (Koes and Camacho, 2012) is a free online service which allows users to search for molecules within the purchasable ZINC database which satisfy pharmacophore criteria, as well as identify pharmacophore features of a molecule.

1.7.7 LigandScout®

LigandScout® (Wolber & Langer, 2005) is a 3D molecular modelling software which is capable of modelling pharmacophoric spaces from protein-ligand complexes as well as

---

[5]Bio-Rad: KnowItAll® Academic Edition. Version 18.0.53 [software]. Available from: https://www.biorad.com/en-mt/product/knowitall-academic-edition-free-chemistry-software?ID=NH29WJ15.

organic molecules. This program aids during the early stages of drug discovery by predicting new structures *in silico* (Wolber & Langer, 2005).

1.7.8 Ligbuilder® v1.2

Ligbuilder® v1.2 (Wang *et al., 2000*) is a Linux® based software which is able to identify the protein's ligand binding pocket and GROW or LINK seed molecules in a manner to occupy the ligand binding pocket.

1.7.9 BIOVIA Draw® v17.1.

BIOVIA Draw® v17.1 [8] is a program that allows users to draw, analyse and edit molecules, chemical processes as well as generate scientific information.

1.8 Aim and Objectives

Literature shows that 6PGD is a viable target for the development of antagonist molecules that could mitigate tumour growth. There is also evidence in literature that parietin is a good lead molecule whose scaffold may be exploited from a drug design perspective for the identification and *de novo* design of novel entities with superior antagonist activity at the 6PGD enzyme with pharmacokinetic properties predisposing to oral bioavailability. Being a component of rhubarb, a widely consumed vegetable, there is also clear evidence that the parietin scaffold is non-toxic.

This literature review consequently makes a case for the aims of this study which are to identify, through VS, and to design *de novo*, novel structures capable of 6PGD modulation that is superior to that of the lead molecule parietin. The optimal structures

---

[8] Dassault Systèmes. BIOVIA Draw. Version 17.1 [software]. Dassault Systèmes. 2017 [cited 2021 Jul 14; downloaded 2021 May 25]. Available from:
https://hts.c2b2.columbia.edu/draw/.

will be identified, further validated, and optimised in preparation for molecular

dynamics studies.

Chapter 2

Methodology

2.2 PDB Deposition

2.2.1 Molecular Modelling & PDB Selection

The parietin scaffold was modelled in SYBYL®-X (Ash *et al*., 2010). The PDB crystallographic deposition 2IZ1 (Sundaramoorthy *et al.,* 2007*)* was chosen describing the *Lactococcus lactis* 6PGD enzyme bound to the small molecule inhibitor PEX. The L*l*6PGD is the preferred variant due to its stable nature when performing crystallographic studies to assess ligand-binding capabilities. From now on, L*l*6PGD will be referred to as 6PDG.
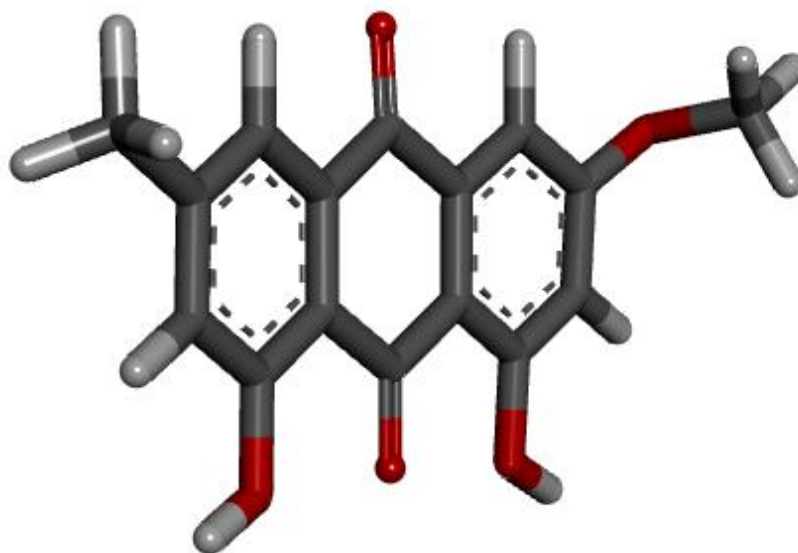
Figure 2.1 The three-dimensional structure of parietin as rendered in BIOVA Discovery Studio Visualizer®.[6]

2.2.2 Extraction of PEX from the 6PGD Enzyme

Using SYBYL®-X (Ash *et al.*, 2010), residues of chain A and PEX were isolated by removing residues of both chains B and C together with all water molecules and irrelevant small molecules present. This process resulted in simplification of later processes as well as allowing for better computational processing. The small molecule inhibitor PEX was extracted from 6PGD chain A as described in the PDB crystallographic deposition 2IZ1 (Sundaramoorthy *et al.,* 2007). Two structures were now generated, the *apo* 2IZ1 and the small molecule PEX in the conformation found when bound to 2IZ1.
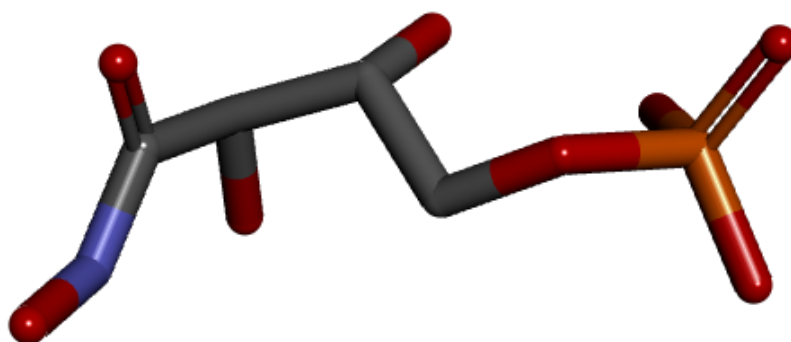
Figure 2.2 The three-dimensional structure of the small molecule inhibitor PEX extracted from the PDB crystallographic deposition 2IZ1 rendered in BIOVA Discovery Studio Visualizer®.[6]

---

[6] Dassault Systèmes. BIOVIA Discovery Studio Visualizer. Version 20.1 [software]. Dassault Systèmes. 2020 [cited 2021 Jul 14; downloaded 2021 May 25]. Available from: https://www.3dsbiovia.com/products/collaborative-science/biovia-discovery-studio/visualization-download.php
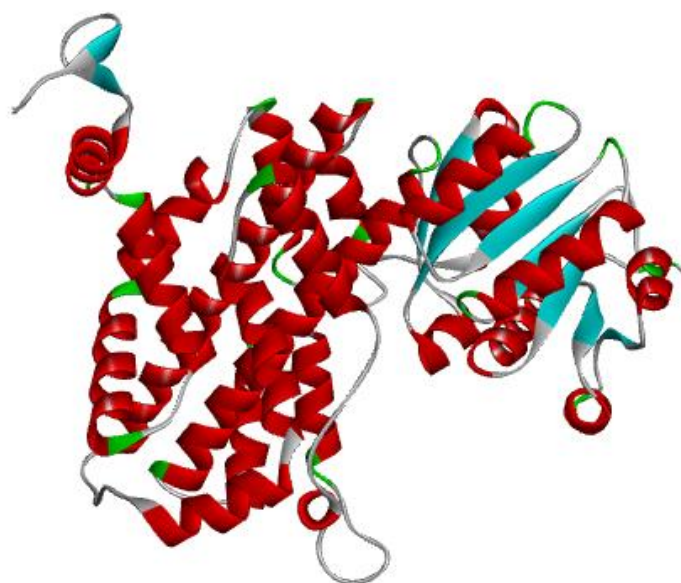
Figure 2.3 The three-dimensional structure of the *apo* form of 6PGD as described the PDB

crystallographic deposition 2IZ1 rendered in BIOVA Discovery Studio Visualizer®.[6]

2.3 Conformational Analysis

2.3.1 Generation of Parietin Conformers

The 'similarity suite' in SYBYL®-X (Ash *et al*., 2010) was used to generate different

conformers of parietin which occupy the *apo* 6PGD's ligand binding pocket. Ring

flexibility was considered. This process resulted in 20 different conformers of parietin

which could occupy the *apo* 6PGD's ligand binding pocket.

---

[6] Dassault Systèmes. BIOVIA Discovery Studio Visualizer. Version 20.1 [software]. Dassault Systèmes.
2020 [cited 2021 Jul 14; downloaded 2021 May 25]. Available from:
https://www.3dsbiovia.com/products/collaborative-science/biovia-discovery-studio/visualization-
download.php

2.3.2 Extraction and estimation of Ligand Binding Energy and Ligand Binding Affinity

The 20 conformers of parietin were numbered and exported as single *.mol2* files. The next step involved the importation of the single conformers into SYBYL®-X (Ash *et al.*, 2010) where their ligand binding energies (LBE) were calculated in kcal mol^{-1} using the 'Energy' function under the 'Compute' section. This process was repeated for all the 20 conformers where an energy profile was generated for each one. This process was used to identify the conformer which had the lowest LBE (kcal mol^{-1}) which would result in better stability when bound to the receptor.

The ligand binding affinity (LBA) in pK$_d$ of each conformer was calculated using X-Score® (Wang et al., 2002). This exercise was carried out to determine the affinity of each of the 19 parietin conformers to the *apo* L*l*6PGD. In this instance, a high LBA (pK$_d$) ensured that the parietin conformer bound strongly to the *apo* L*l*6PGD's ligand binding pocket.

2.3.3 Determination of the optimal conformers

The values of the LBE (kcal mol^{-1}) and LBA (pK_d) of each of the 20 conformers of parietin were inputted into a Microsoft Excel[7] spreadsheet. A graph was then plotted with the LBE (kcal mol^{-1}) and LBA (pK_d) of the 20 conformers on the y-axis and the corresponding conformer number on the x-axis. The optimal conformer of parietin was chosen based on the peak height difference between LBE (kcal mol^{-1}) and LBA (pK_d). This reasoning was based on the notion that a low LBE (kcal mol^{-1}) and a high LBA (pK_d) would provide with the most stable conformer of parietin.

---

[7] Microsoft Corporation. Microsoft Excel [Internet]. 2018. Available from:
https://office.microsoft.com/excel

2.4 Virtual Screening

2.4.1 Pharmacophore Generation

LigandScout® (Wolber & Langer, 2005) was used to analyse the critical interactions between the optimal conformer of parietin and L/6PGD. Due to the structural diversity between the bound small molecule inhibitor PEX to L/6PGD as described in the PDB crystallographic deposition 2IZ1 and the optimal conformer of parietin, a consensus pharmacophore between the two could not be formed.
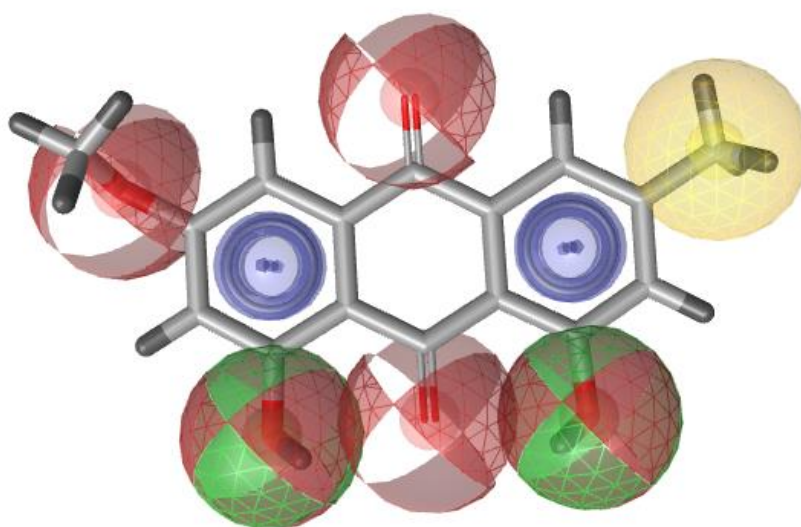

Figure 2.4 The general pharmacophore of the optimal conformer of parietin as rendered in LigandScout® (Wolber & Langer, 2005).

2.4.2 Screening Hit Molecules & Filtration

The resultant general pharmacophore was imported onto the online database ZincPharmer® (Koes and Camacho, 2012) for virtual screening of analogous molecules. Various filters were employed to ensure that the nature of the resultant molecules was lead-like.

The filters applied initially were:

- Maximum total number of hits: 300

- Maximum root mean squared deviation (RMSD): 1

- $1 \leq$ molecular weight ≤ 300

- $1 \leq$ rotatable bonds ≤ 3

These filters resulted in no hits and the maximum molecular weight was increased to 500 whilst the maximum numbers of rotatable bonds were increased to 5. This process resulted in 4 hit molecules.

2.4.3 Identification of Lipinski-Rule Compliant Hits

A filtration exercise was carried out using the program MONA® (Hilbig & Rarey, 2015) to identify which of the resultant hits obtained in section 2.4.2. For the hits to be Lipinski-Rule complient, the following criteria was to be met:

- Hydrogen donors: 1-5

- Hydrogen acceptors: 1-10

- LogP: 1 - 5

- Molecular weight: 0-500

All 4 hits were identified as Lipinski-Rule compliant (Lipinski et al, 2001)and were exported as a single file which incorporated all 4 hit structures in *.mol2* format.

2.4.4 ProtoMol Generation

The PDB crystallographic deposition 2IZ1 (Sundaramoorthy *et al.,* 2007*)* was imported into SYBYL®-X (Ash *et al*., 2010) using the in-built 'SurflexDocking' suite and a process similar to that done in section 2.2.2 was made, where there was removal of both chains B and C as well as all water molecules present and small molecules. This process resulted in the *apo* form of the L*l*6PGD enzyme where an exercise to model the ProtoMol representing the energetically unstable amino acids at the core of the L*l*6PGD enzyme. After the ProtoMol was generated, the *.mol2* file created in section 2.4.3 was imported whilst still in the 'SurflexDocking' suite. The results of this exercise were saved and a table describing their affinities was created.
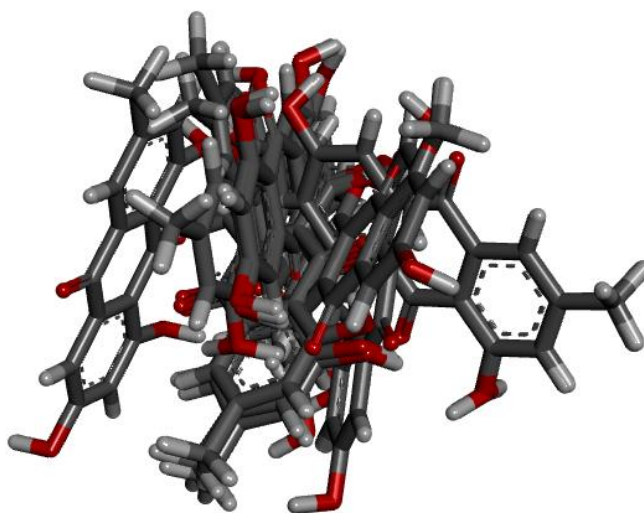
Figure 2.5 The three-dimensional structure 4 hit molecules occupying the ProtoMol of L*l*6PGD as described the PDB crystallographic deposition 2IZ1 rendered in BIOVA Discovery Studio Visualizer®.[6]

2.5 The *de novo* Approach – Structure Based Drug Design

2.5.1 Generation of a 2D Topology Map

The *de novo* approach to drug design required the use of the previously generated *apo* L*l*6PGD in 2.2.2 was used in this stage of the study. The first step was to generate a 2D topology map of the critical interactions between the optimal conformer of parietin and the L*l*6PGD active site. Both the *apo* L*l*6PGD and the optimal conformer of parietin were imported in SYBYL®-X (Ash *et al*., 2010) keeping the same spatial orientation and merged together into a single *.mol2* file. The resultant *.mol2* file was imported into BIOVA Discovery Studio Visualizer[6] were the optimal conformer of parietin was chosen as the ligand and the *apo* L*l*6PGD was chosen as a receptor, all done in the 'Receptor-Ligand Interactions' window. A 2D topology map was then generated and saved as a *.png* image.

2.5.2 Generation of Seed Molecules

The optimal conformer of parietin was chosen as a scaffold to be modified in SYBYL®-X to create seed molecules to be used in LigBuilder v1.2 (Wang *et al.,* 2000) which runs on a Linux® based operating system Ubuntu®. Using the 2D topology map generated, atoms contributing to unfavourable ligand-protein interactions were targeted to be modified inside SYBYL®-X. These atoms were changed into special hydrogen atoms (*H.spc*) to direct molecular growth. LigBuilder v1.2 (Wang *et al.,* 2000) is able to identify the *H.spc* and carry out respective GROW and LINK functions on the seeds created.

2.5.3 *De novo* Drug Design

In LigBuilder v1.2 (Wang *et al.,* 2000) the POCKET module was used to virtually model the ligand binding pocket of L*l*6PGD. For this, the *apo* L*l*6PGD was used, and a hypothetical ligand-binding pocket was created where the necessary GROW and LINK algorithms would work.

Successful GROW and LINK operations resulted in two separate file outputs, *population.lig* and *ligands.lig*. Both these files were used in the PROCESS function of LigBuilder v1.2 (Wang *et al.,* 2000) which selected the best results from the GROW and LINK functions.

An 'INDEX' file which contained technical results regarding the output molecules was created. Data from the 'INDEX' file was imported into Microsoft® Excel® and the molecules were filtered according to Lipinski's rules. Molecules having a molecular weight of less than 500 and a LogP of less than 5 were kept and as a result. The resultant *.mol2* files were converted into *.sd* files and further converted into *.mol* files which were able to be read by BIOVA® Draw[8]. The latter program was used to calculate the amount of Hydrogen Bond Acceptors and Hydrogen Bond Donors of a selection of the resultant molecules which needed to be not more than 10 Hydrogen Bond Acceptors and not more than 5 Hydrogen Bond Donors.

---

[8] Dassault Systèmes. BIOVIA Draw. Version 17.1 [software]. Dassault Systèmes. 2017 [cited 2021 Jul 14; downloaded 2021 May 25]. Available from:
https://hts.c2b2.columbia.edu/draw/
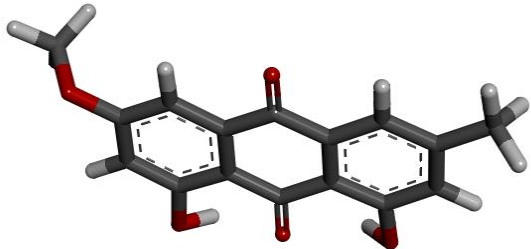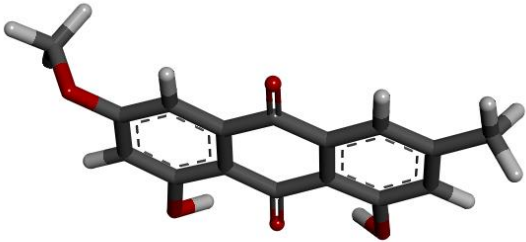
Chapter 3
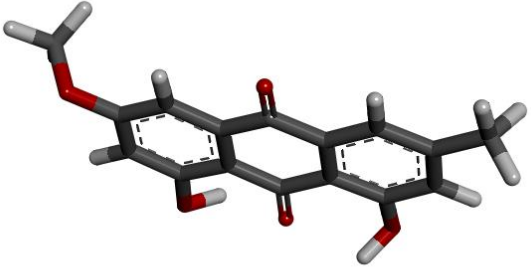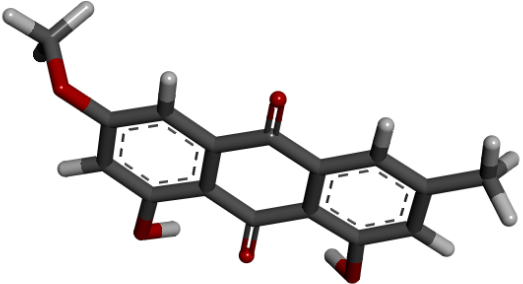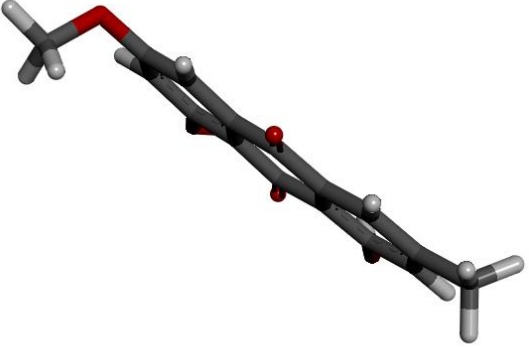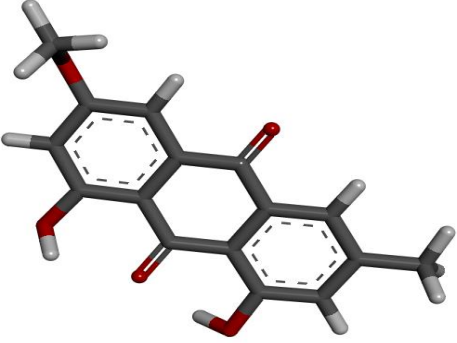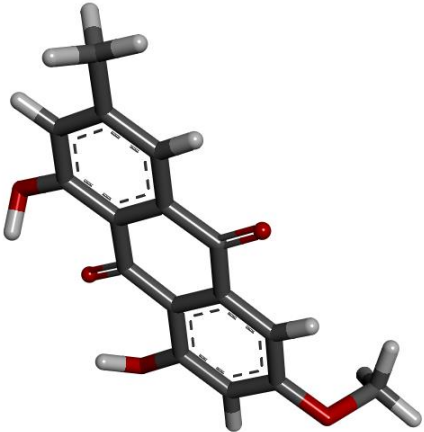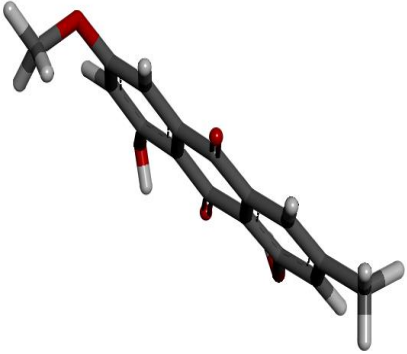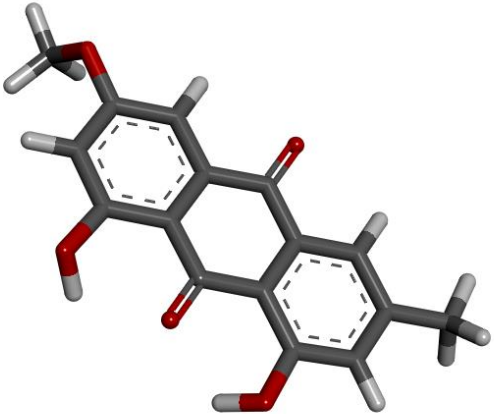
Results

3.1 Virtual Screening Results
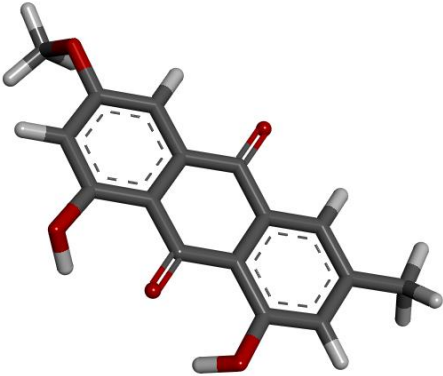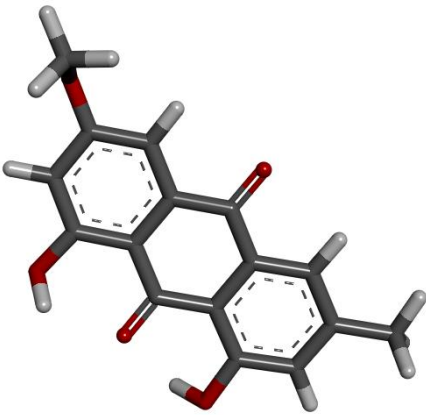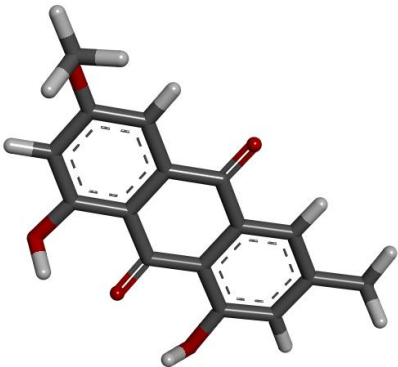
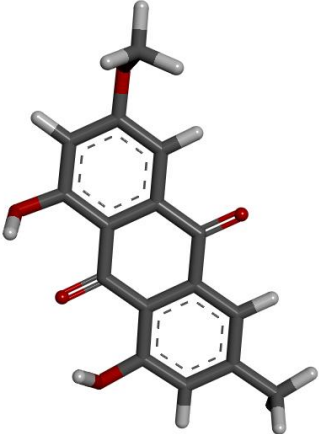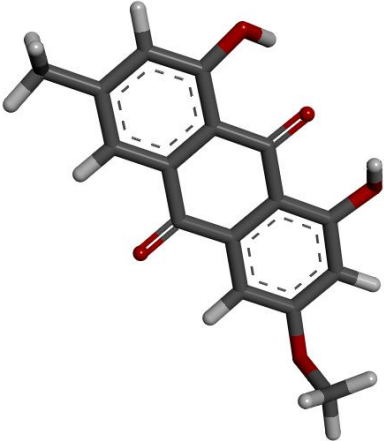**3.1.1 Conformers of Parietin and *in silico* Calculations**
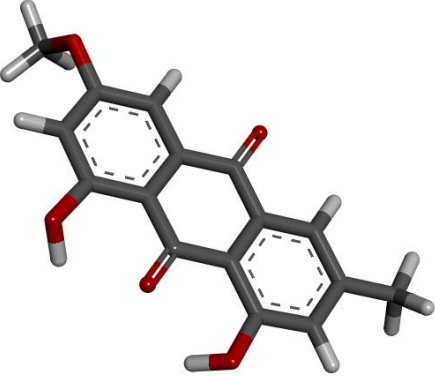
The respective ligand binding energies (LBEs) (kcalmol^{-1}) and ligand binding affinities

(LBAs) of each conformer were generated in this step. SYBYL®-X was used to generate

the LBEs while the program x-Score® (Wang et al., 2002) was used to compute the LBAs
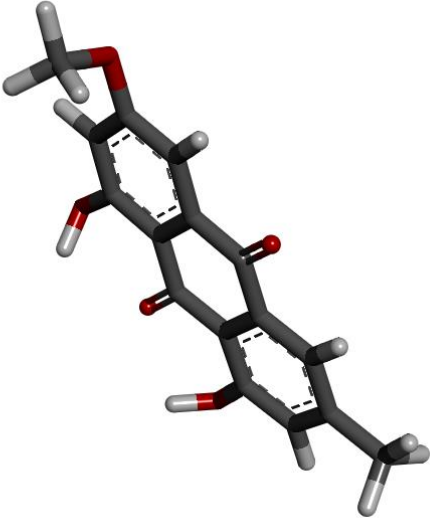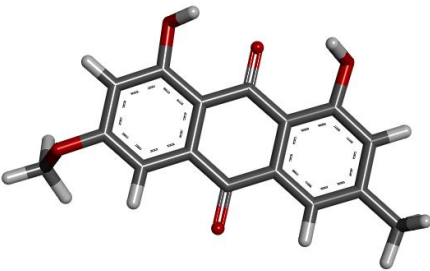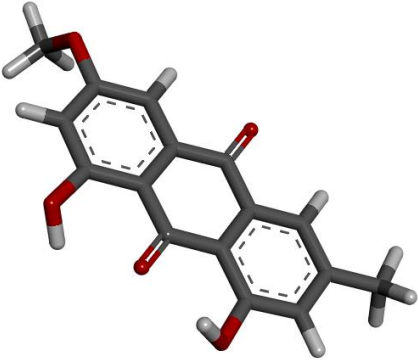
of the 20 conformers.

Conformer Number	Conformer	Ligand Binding Affinity (pK_d)	Ligand Binding Energy (kcalmol^{-1})
0		4.25	50.796
1		4.26	49.824

2		4.3	49.934
3		4.3	49.952
4		4.63	49.81
5		4.9	49.853

6		4.67	50.602
7		4.62	49.92
8		4.21	49.884

9		4.22	49.862
10		4.94	49.813
11		5.09	49.921

12		4.33	49.901
13		4.85	50.953
14		5.06	49.793

15		4.58	49.923
16		4.3	49.872
17		4.3	49.932
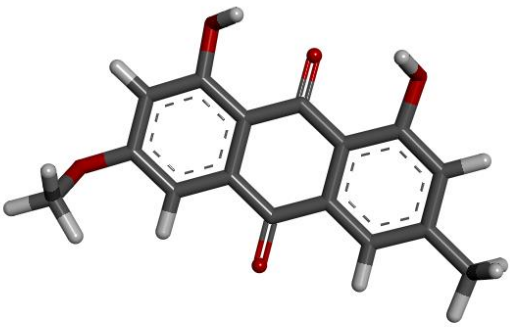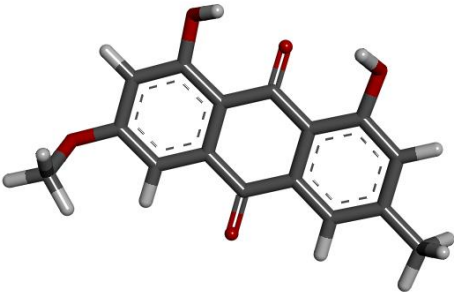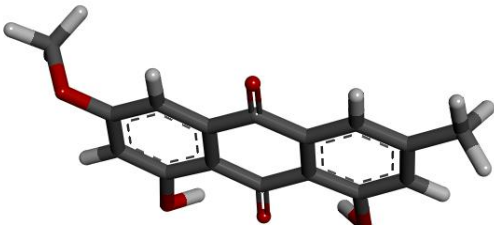
18		4.72	50.635
19		4.73	50.622
J		4.25	50.796

Table 3.1 The 20 different conformers of parietin inside the 6PGD ligand binding pocket rendered in

Discovery Studio Visualizer®.[6]

[6] Dassault Systèmes. BIOVIA Discovery Studio Visualizer. Version 20.1 [software]. Dassault Systèmes. 2020 [cited 2021 Jul 14; downloaded 2021 May 25]. Available from: https://www.3dsbiovia.com/products/collaborative-science/biovia-discovery-studio/visualization-download.php.

3.1.2 Selection of the optimal conformer of Parietin

Results obtained from the conformational analyses were plotted in a graph. The graph describes the Ligand Binding Energy (LBE) versus Ligand Binding Affinity (LBA) of the 20 conformers of parietin with the optimal conformer circled. The optimal conformer was chosen as having the lowest LBE and highest LBA.
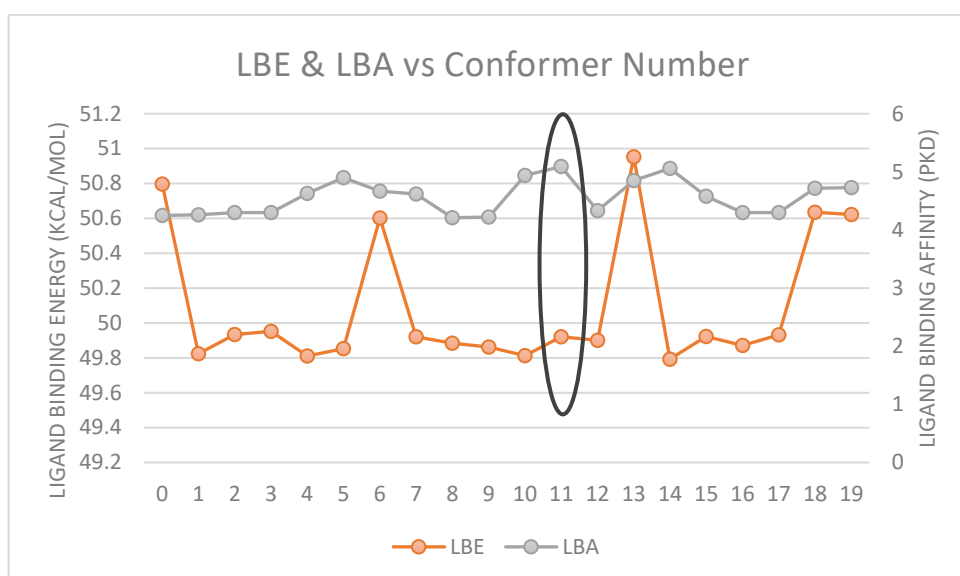
Figure 3.1 A graph of Ligand Binding Energy (LBE) versus Ligand Binding Affinity (LBA) of the 20 conformers of parietin with the optimal conformer circled.

3.1.3 Virtual Screening Results

Virtual screening using ZincPharmer® (Koes and Camacho, 2012) resulted in 4 hits. These 4 hits were docked inside the protomol designed in section 2.4.4 and the resultant affinities were tabulated as seen Table 3.1

ZincPharmer® ID	Popular Name	Affinity (pK_d)
ZINC06070262	Endocrocin	2.92
ZINC05461939	Catenarin	2.58
ZINC03978794	Parietin	2.32
ZINC03824868	Emodin	1.91

Table 3.2 Table of the four hits obtained through virtual screening together with their respective popular name and affinity to the *apo* form of the 6PGD receptor.
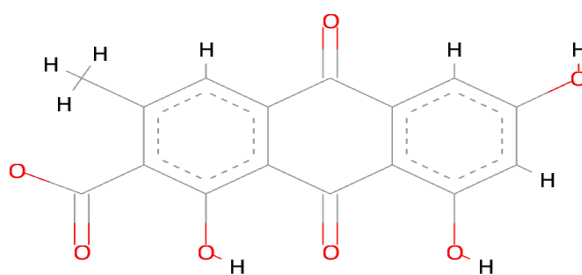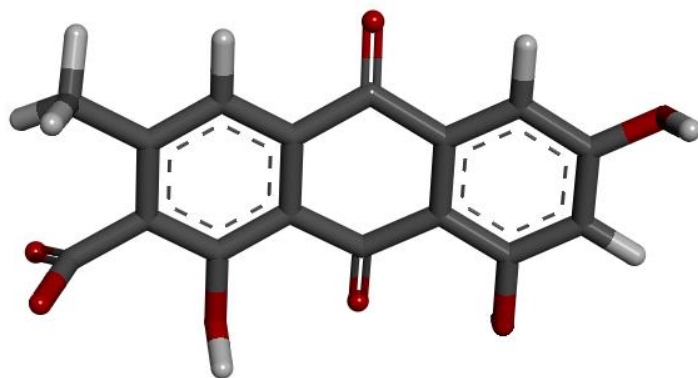
Figure 3.2 ZINC06070262 molecule rendered using BIOVA Discovery Studio Visualizer®.[6]
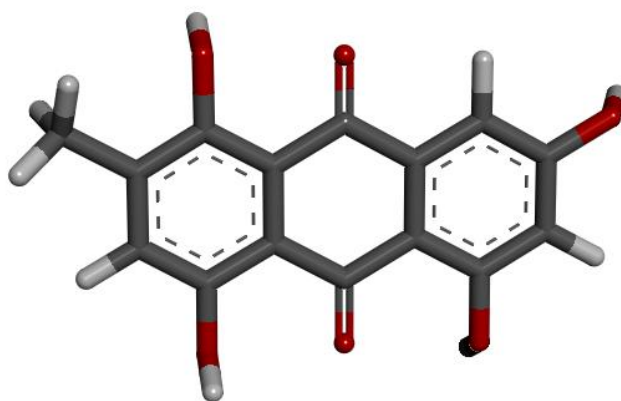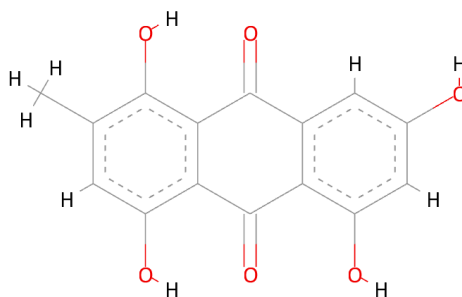
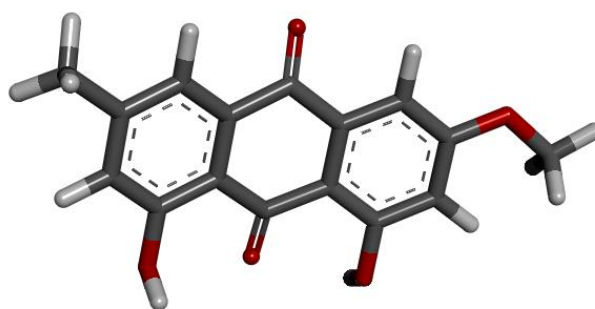**Figure 3.3** ZINC05461939 molecule rendered using BIOVA Discovery Studio Visualizer®[6].
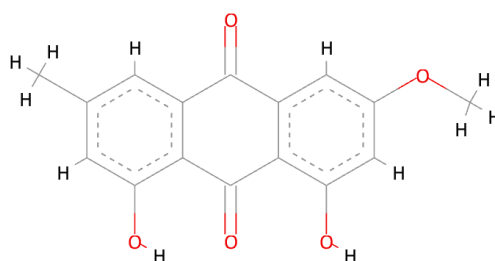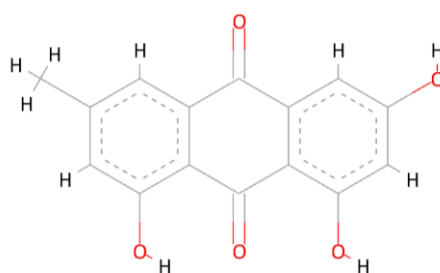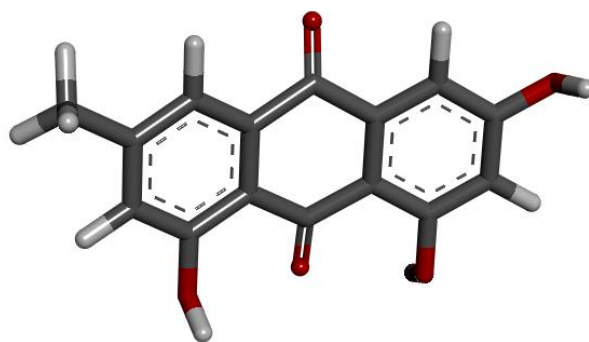

Figure 3.4 ZINC03978794 molecule rendered using BIOVA Discovery Studio Visualizer®.[6]

[6] Dassault Systèmes. BIOVIA Discovery Studio Visualizer. Version 20.1 [software]. Dassault Systèmes. 2020 [cited 2021 Jul 14; downloaded 2021 May 25]. Available from: https://www.3dsbiovia.com/products/collaborative-science/biovia-discovery-studio/visualization-download.php.

Figure 3.5 ZINC03824868 molecule rendered using BIOVA Discovery Studio Visualizer®.[6]

[6] Dassault Systèmes. BIOVIA Discovery Studio Visualizer. Version 20.1 [software]. Dassault Systèmes. 2020 [cited 2021 Jul 14; downloaded 2021 May 25]. Available from: https://www.3dsbiovia.com/products/collaborative-science/biovia-discovery-studio/visualization-download.php.

3.2 *De Novo* Results

3.2.1 Structure activity relationship between the optimal conformer of parietin and the ligand binding pocket of the *apo* 6PGD receptor
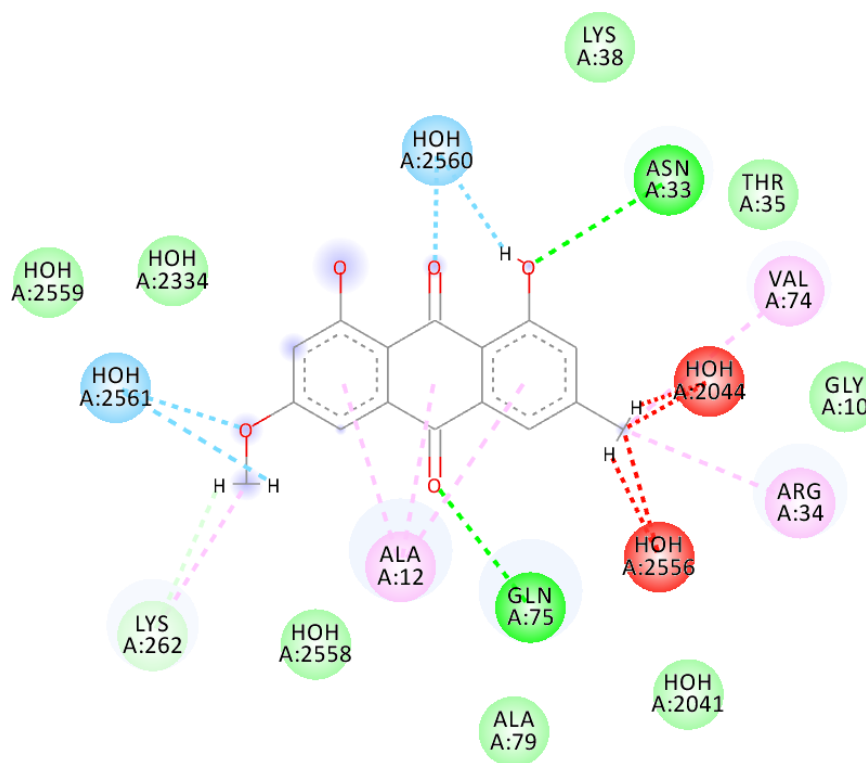
Figure 3.6 The 2D topology map showing critical interactions between the optimal conformer of parietin and the 6PGD receptor rendered in BIOVA Discovery Studio Visualiser®.[6]

---

[6] Dassault Systèmes. BIOVIA Discovery Studio Visualizer. Version 20.1 [software]. Dassault Systèmes. 2020 [cited 2021 Jul 14; downloaded 2021 May 25]. Available from: https://www.3dsbiovia.com/products/collaborative-science/biovia-discovery-studio/visualization-download.php.

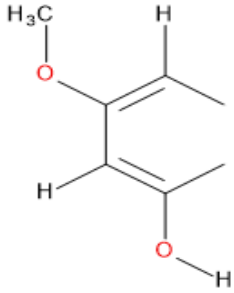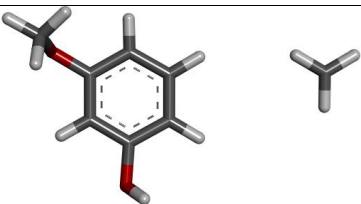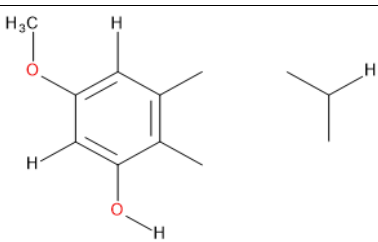## 3.2.2 Seed Generation using the Optimal Conformer of Parietin
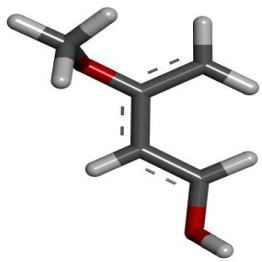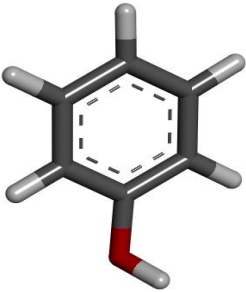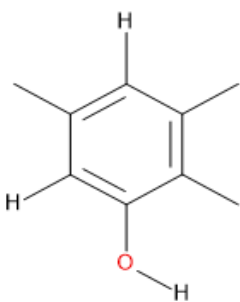
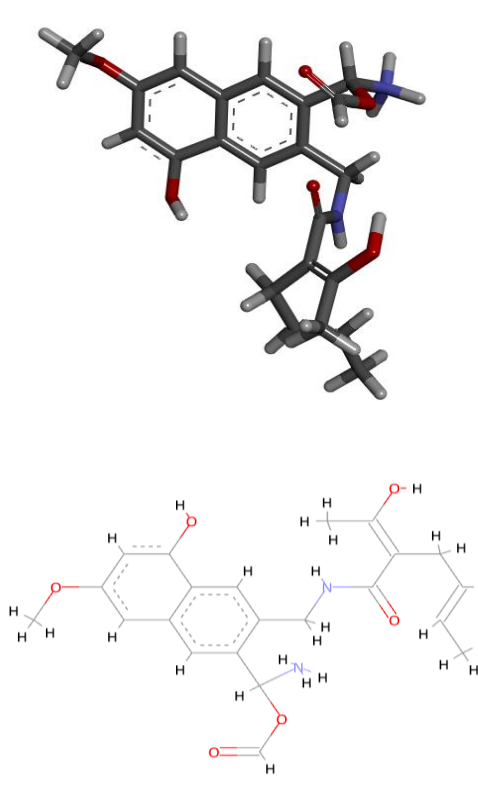| Seed	Process	Structure in 3D	Structure in 2D
Seed 1	GROW		
Seed 2	LINK		
Seed 3	GROW		

Table 3.3 The 3 seeds which generated successful molecules that occupy the 6PGD receptor. 3D molecules rendered using BIOVA Discovery Studio Visualiser®[6] and 2D molecules were rendered using BIOVA Draw®.[8]
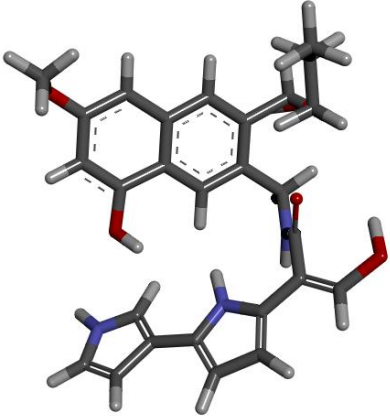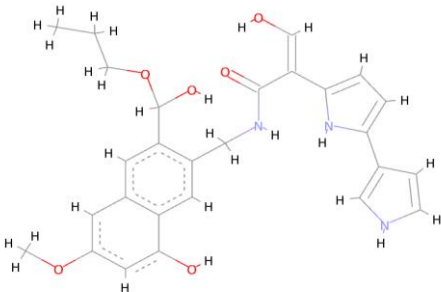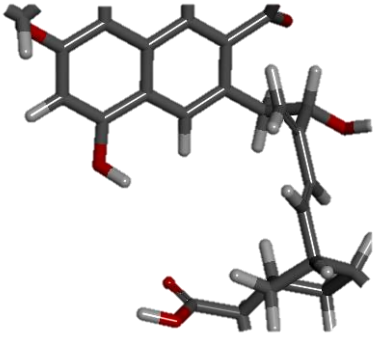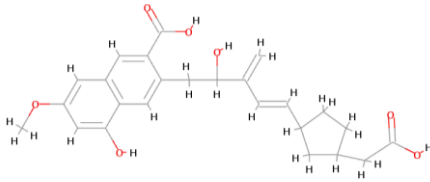
[6] Dassault Systèmes. BIOVIA Discovery Studio Visualizer. Version 20.1 [software]. Dassault Systèmes. 2020 [cited 2021 Jul 14; downloaded 2021 May 25]. Available from: https://www.3dsbiovia.com/products/collaborative-science/biovia-discovery-studio/visualization-download.php.
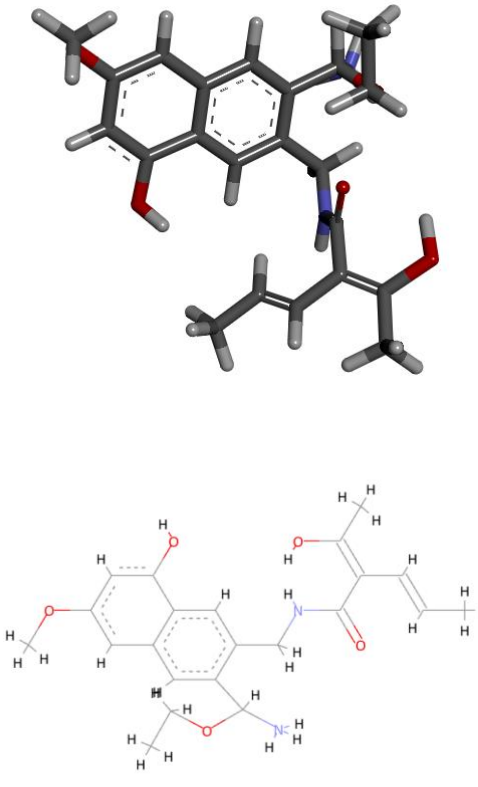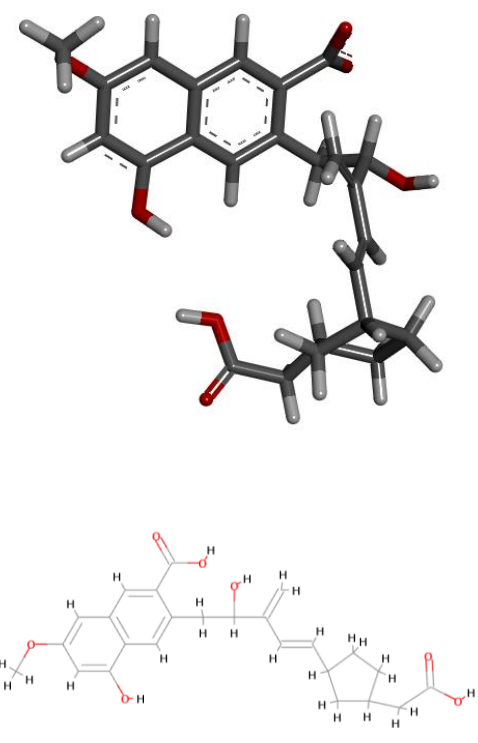
[8] Dassault Systèmes. BIOVIA Draw. Version 17.1 [software]. Dassault Systèmes. 2017 [cited 2021 Jul 14; downloaded 2021 May 25]. Available from: https://hts.c2b2.columbia.edu/draw/.
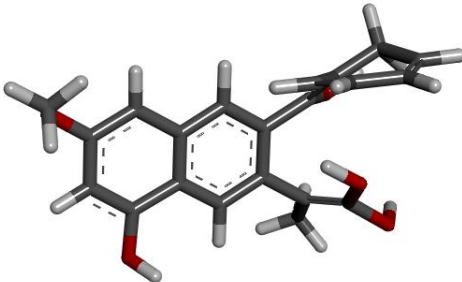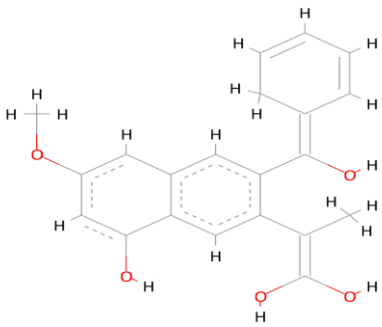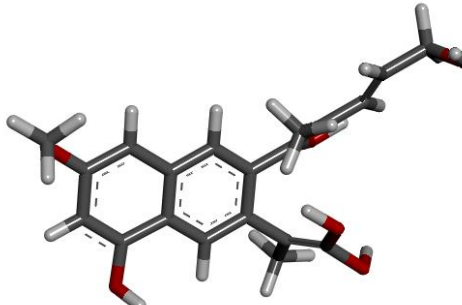
Both Seed 1 and Seed 3 resulted in 200 molecules after which filtering for Lipinski Rule compliance resulted in 164 and 165 molecules respectively. Seed 2 resulted in 10 molecules only which 'molecule 10' was correctly linked to form a complete molecule which satisfied Lipinski's Rule of 5 Criteria (Lipinski et al, 2001) as stated below;

- Molecular weight < 500

- LogP ≤ 5

- Hydrogen bond acceptors ≤ 10

- Hydrogen bond donors ≤ 5

Molecule ID	Structure and Family	Properties
6	 Family 2	Molecular Weight: 415 LogP: 3.07 Affinity (pK_d): 8.3 Hydrogen Bond Acceptors: 6 Hydrogen Bond Donors: 4

8	Family 2	Molecular Weight: 491 LogP: 3.51 Affinity (pK_d): 7.8 Hydrogen Bond Acceptors: 6 Hydrogen Bond Donors: 4
67	Family 3	Molecular Weight: 439 LogP: 3.84 Affinity (pK_d): 7.57 Hydrogen Bond Acceptors: 7 Hydrogen Bond Donors: 4

9		Molecular Weight: 401
		LogP: 3.15
		Affinity (pK_d): 7.5
		Hydrogen Bond Acceptors: 5
		Hydrogen Bond Donors: 4
	Family 2	
68		Molecular Weight: 439
		LogP: 3.84
		Affinity (pK_d): 7.43
		Hydrogen Bond Acceptors: 7
		Hydrogen Bond Donors: 4

	Family 3	
190		Molecular Weight: 352 LogP: 4.55 Affinity (pK_d): 5.45 Hydrogen Bond Acceptors: 4 Hydrogen Bond Donors: 5
	Family 5	
191		Molecular Weight: 358 LogP: 3.33 Affinity (pK_d): 5.45 Hydrogen Bond Acceptors: 6 Hydrogen Bond Donors: 5

	  Family 5	
192	 Family 5	Molecular Weight: 358 LogP: 4.27 Affinity (pK_d): 5.45 Hydrogen Bond Acceptors: 6 Hydrogen Bond Donors: 4

Table 3.4 The 5 molecules with the highest affinity with the worst 3 molecules generated with seed 25.

3D and 2D molecules rendered using BIOVA Discovery Studio Visualiser®.[6]

---

[6] Dassault Systèmes. BIOVIA Discovery Studio Visualizer. Version 20.1 [software]. Dassault Systèmes. 2020 [cited 2021 Jul 14; downloaded 2021 May 25]. Available from:

Molecule ID	Structure and Family	Properties
10	 Family 5	Molecular Weight: 331 LogP: 3.94 Affinity (pK_d): 5.03 Hydrogen Bond Acceptors: 4 Hydrogen Bond Donors: 1
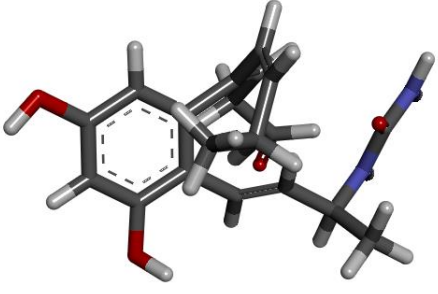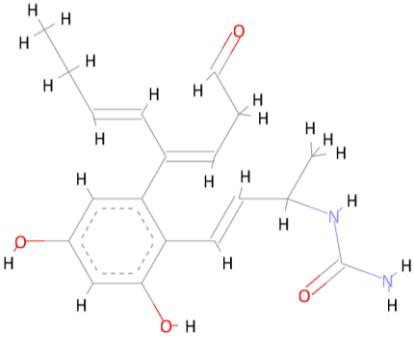
Table 3.5: The only valid molecule generated with seed 2. 3D and 2D molecules rendered using BIOVA

Discovery Studio Visualiser®.[6]

https://www.3dsbiovia.com/products/collaborative-science/biovia-discovery-studio/visualization-download.php.

[6] Dassault Systèmes. BIOVIA Discovery Studio Visualizer. Version 20.1 [software]. Dassault Systèmes. 2020 [cited 2021 Jul 14; downloaded 2021 May 25]. Available from: https://www.3dsbiovia.com/products/collaborative-science/biovia-discovery-studio/visualization-download.php.

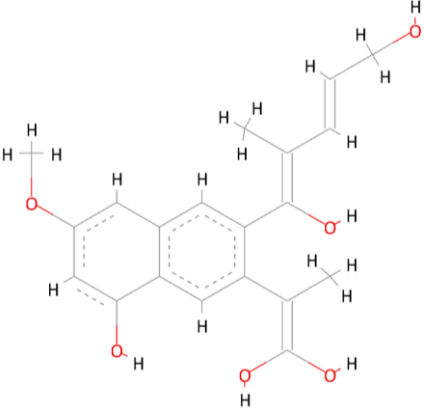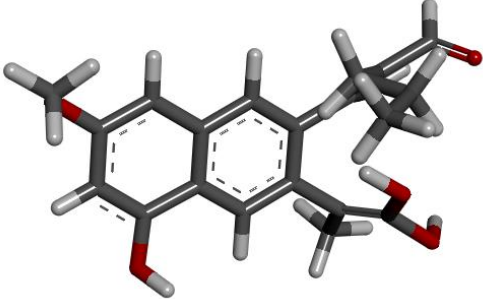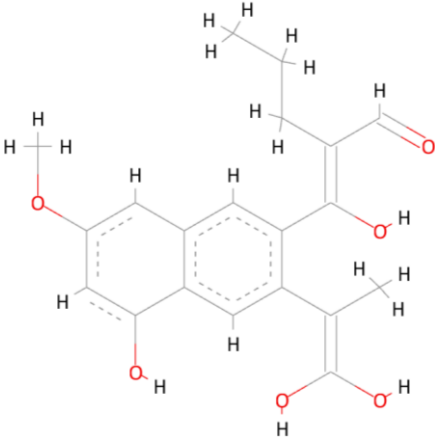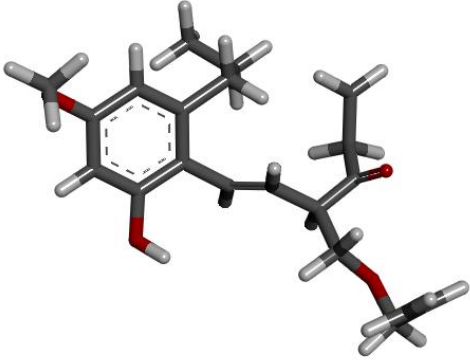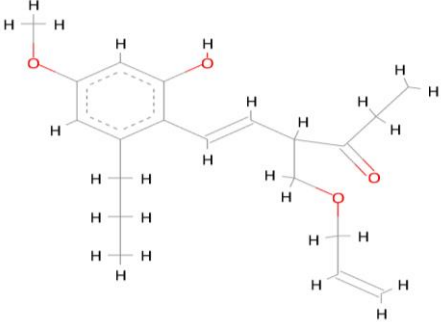| Molecule ID	Structure and Family	Properties
001	 Family 1	Molecular Weight: 344 LogP: 3.36 Affinity (pK_d): 7.96 Hydrogen Bond Acceptors: 4 Hydrogen Bond Donors: 4
002		Molecular Weight: 399 LogP: 3.81 Affinity (pK_d): 7.83 Hydrogen Bond Acceptors: 5 Hydrogen Bond Donors: 4

Family 1 | |
| 003 |

Family 1 | Molecular Weight: 315

LogP: 3

Affinity (pK_d): 7.82

Hydrogen Bond Acceptors: 4

Hydrogen Bond Donors: 4 |

101		Molecular Weight: 382
		LogP: 4.87
		Affinity (pK_d): 7.54
		Hydrogen Bond Acceptors: 4
		Hydrogen Bond Donors: 3
	Family 3	
102		Molecular Weight: 369
		LogP: 4.87
		Affinity (pK_d): 7.54
		Hydrogen Bond Acceptors: 2
		Hydrogen Bond Donors: 3

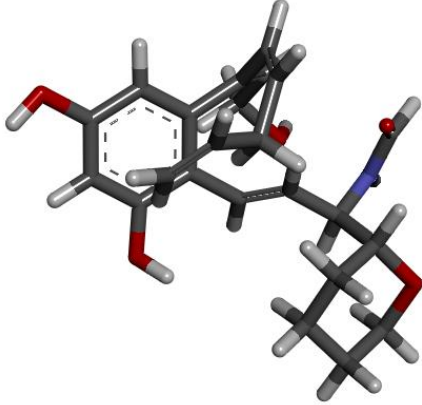|	Family 3	
083	 Family 2	Molecular Weight: 352 LogP: 4.55 Affinity (pK_d): 5.45 Hydrogen Bond Acceptors: 3 Hydrogen Bond Donors: 3
081		Molecular Weight: 393 LogP: 3.53 Affinity (pK_d): 6.03 Hydrogen Bond Acceptors: 3 Hydrogen Bond Donors: 3
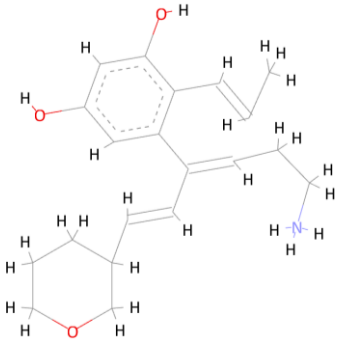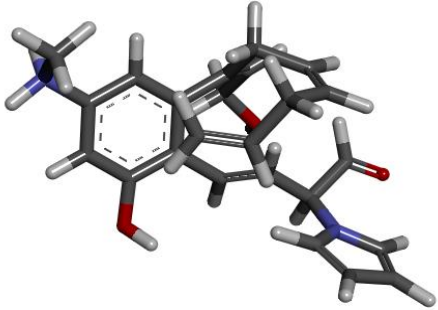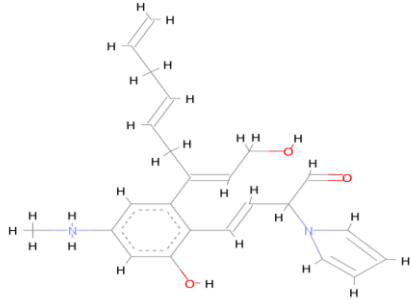
	Family 1	
143	Family 4	Molecular Weight: 393 LogP: 4.72 Affinity (pK_d): 6.03 Hydrogen Bond Acceptors: 3 Hydrogen Bond Donors: 3

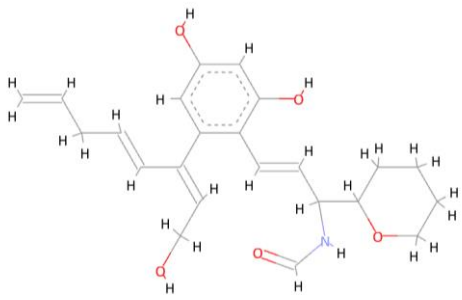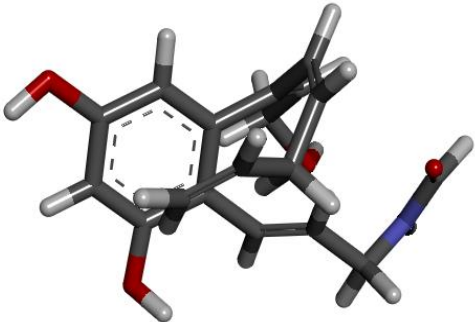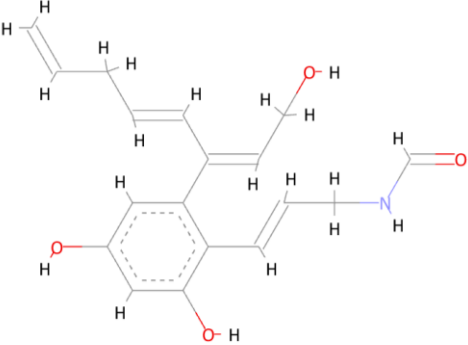**Table 3.6** The 5 molecules with the highest affinity with the worst 3 molecules generated with seed 3.

3D and 2D molecules rendered using BIOVA Discovery Studio Visualiser®.[6]

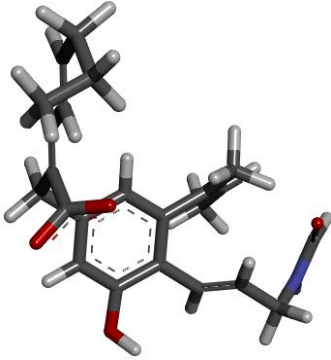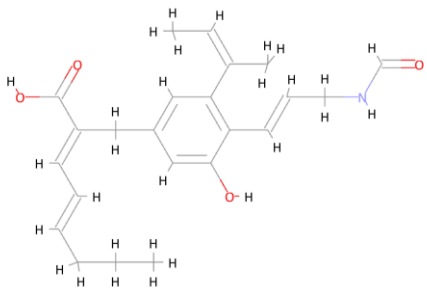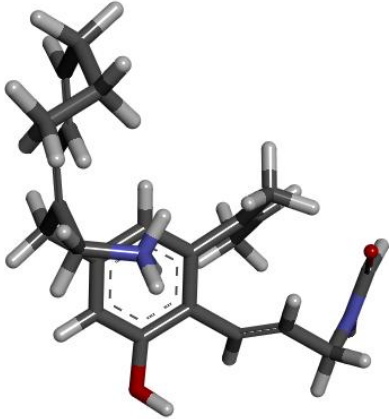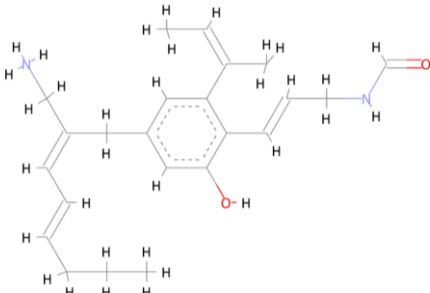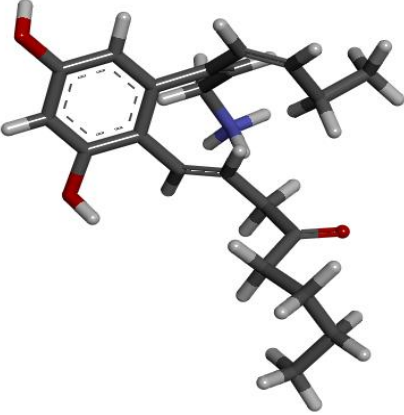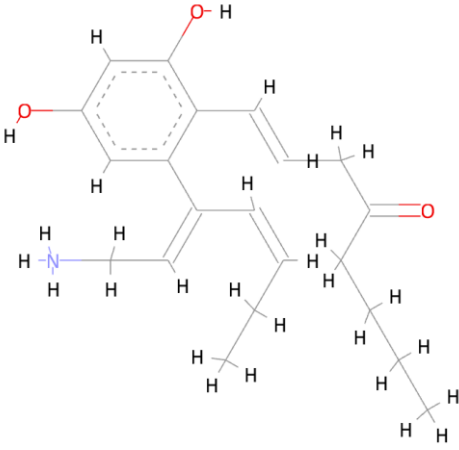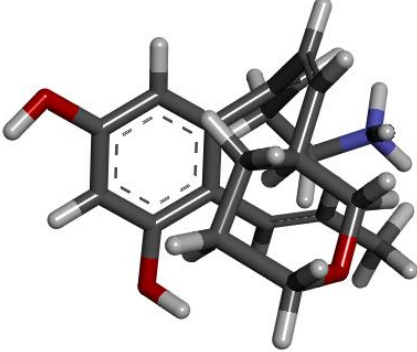[6] Dassault Systèmes. BIOVIA Discovery Studio Visualizer. Version 20.1 [software]. Dassault Systèmes. 2020 [cited 2021 Jul 14; downloaded 2021 May 25]. Available from: https://www.3dsbiovia.com/products/collaborative-science/biovia-discovery-studio/visualization-download.php.

Chapter 4

Discussion

Inhibition of 6PGD yielded promising results in decreasing the rate of progression and size of tumours. This study explored the possibility of optimising the parietin scaffold by identifying already known molecules which could similarly modulate the 6PGD receptor through virtual screening and by designing new molecules *de novo* capable of occupying and modulating the 6PGD ligand binding pocket based on its interactions with parietin.

Using the optimal conformer of parietin as a general pharmacophore, virtual screening produced 4 structurally similar hits capable of interaction with the 6PGD receptor. All 4 hit molecules were Lipinski Rule compliant (Lipinski et al, 2001) meaning that they would be suitable candidates for further development. The affinity of each of the 4 hits was calculated using a docking exercise using a protomol generated inside SYBYL®-X (Ash *et al.*, 2010). All 4 hits from virtual screening showed similar affinity, with endocrocin and catenarin, both secondary metabolites having a slightly higher affinity for the 6PGD receptor. Thus far these latter molecules have not been investigated for anti-tumour properties which presents with the opportunity for further investigation. Emodin on the other hand, has been associated (Gu *et al.,* 2019) with some anti-tumour properties.

In the *de novo* approach, each seed structure could be described as a pharmacophore (P1) which was created using SYBYL®-X (Ash *et al.*, 2010) with reference being made to the previously created topology maps. The process was consequently user driven unlike the creation of pharmacophore 2 (P2) which was computer generated. This latter will be the basis of this discussion.

The *virtual screening* approach differs from *de novo* design in the sense that pharmacophoric space is not restrictive allowing for new growth beyond the bioactive ligand binding pocket typically modelled during *de novo* design. Attempts at producing

a consensus pharmacophore involving the parietin scaffold were not successful. Consequently, a pharmacophore based on the parietin scaffold alone was used to probe the ZINC Pharmer® (Koes and Camacho, 2012) database. Virtual screening as a process is pharmacophore based and consequently allows for identification of hits which as long as they conform to the pre-designated pharmacophoric features, can be structurally very diverse. In this case however, only 4 Lipinski Rule compliant hits that were structurally very similar were obtained. The protomol is based on the vacant space found on the receptor surface the extent of its bioactivity cannot be determined computationally. In the *de* novo approach however, because of spatial limitations, there is less room for innovation. There is however, a greater chance of bioactivity owing to the fact that *de novo* growth is carried out within a pharmacophoric space that was crystallographically described (in this case pdb crystallographic deposition 2IZ1) as being bioactive. The GROW and LINK functions were subsequently used to drive molecular growth using the seed structures, creating new molecule outputs which occupy and interact with the *apo* L*l*6PGD ligand binding pocket. The outputs were divided into families which are essentially a pharmacophore of the newly generated molecules. Both Seed 1 and Seed 3 were based on the same ring structure having *H.spc*s at different *loci* and producing 200 molecules using the GROW function. In both Seeds 1 and 3 the molecule with the highest affinity is structurally compared to that of lowest affinity from each family. A total of 8 families were created with Seed 1 with family 2 having the highest set of affinities with the highest being 8.3 kcal mol^{-1}. Seed 3 had a total of 200 molecules which resulted in 13 families. The molecule with the highest affinity is molecule 1 which had an affinity of 7.94 kcal mol^{-1}.

Each seed structure could be described as a pharmacophore (P1) which can be shown in Table 4.1, which were created using SYBYL®-X (Ash *et al.*, 2010) according to the topology map created previously. The process is thus user driven unlike the creation of pharmacophore 2 (P2) which is computer generated.
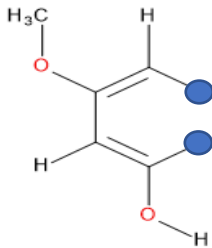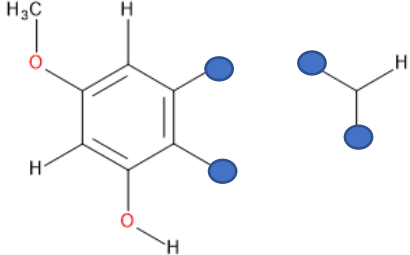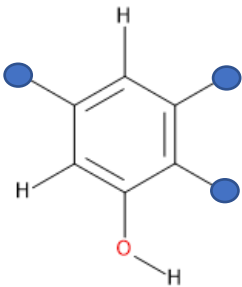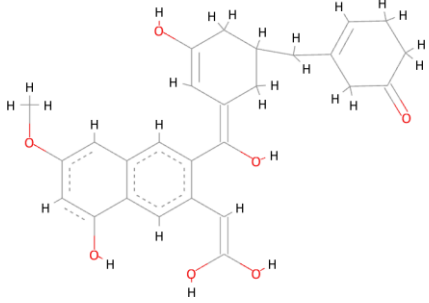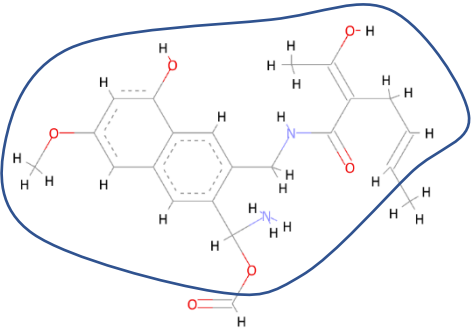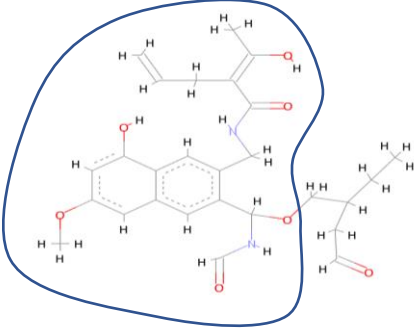
Seed Number	Process	Pharmacophore (P1)
1	Grow	
2	Link	
3	Grow	

Table 4.1 Showing the structure of the modelled seeds. The blue circles represent *H.spc* atoms which were added using SYBYL®-X (Ash *et al.*, 2010) to direct molecular growth in LigBuilder v1.2 (Wang *et al.*, 2000). 2D molecules were rendered in BIOVIA Draw®[8].

---

[8] Dassault Systèmes. BIOVIA Draw. Version 17.1 [software]. Dassault Systèmes. 2017 [cited 2021 Jul 14; downloaded 2021 May 25]. Available from:https://hts.c2b2.columbia.edu/draw/.

Family	Optimally Binding	Molecular Structure Exhibiting the Lowest Affinity
1	Molecule 001 Affinity (p*K*d): 6.33	Only one molecule was left in this family after filtering for Lipinski Rule Compliance.
A comparison could not be made as there was only one molecule was left after filtering for Lipinski Rule Compliance.		
2	Molecule 006 Affinity (p*K*d): 8.3	Molecule 066 Affinity (p*K*d): 5.48
The extended sidechain in molecule 066 may be blocking it from completely occupying the ligand binding pocket.		
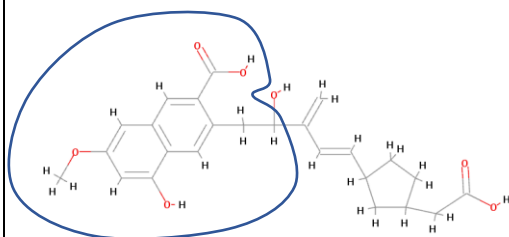
3	Molecule 67 Affinity (pKd): 7.57	Molecule 87 Affinity (pKd): 5.65
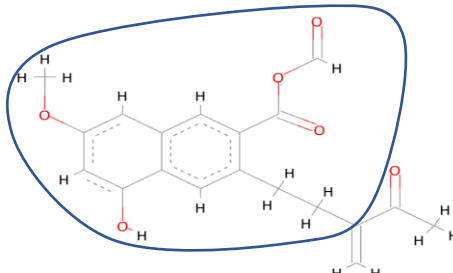
Molecule 67 has a longer and more robust side chain than molecule 87. In molecule 67, the cyclopentane ring and the carboxyl group may contribute to a better binding affinity.
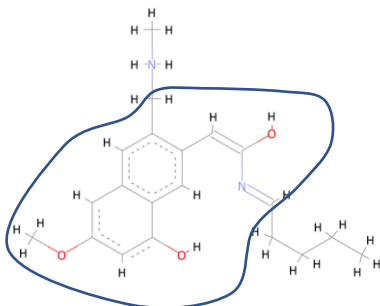
4	Molecule 88 Affinity(pKd): 7.18	Molecule 102 Affinity(pKd): 5.7
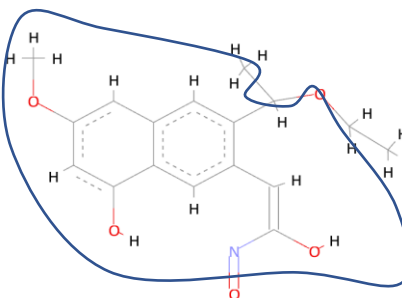
Molecule 102 lacks robustness due to the short side chains as compared to molecule 88
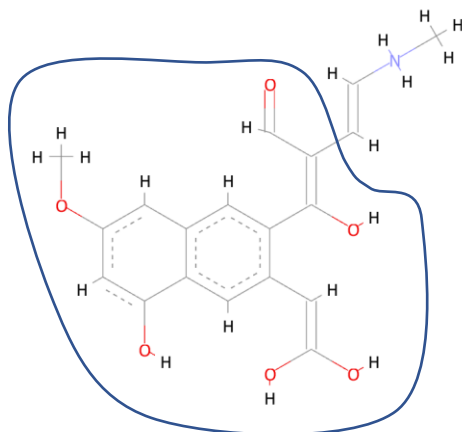
5	Molecule 106 Affinity (pKd): 7.07	Molecule 192 Affinity (pKd): 5.45
In Molecule 106 the sidechain involving an amino group may contribute to better binding affinity where nitrogen may act as an H-bond acceptor		
6	Molecule 193 Affinity (pKd): 6.62	Molecule 194 Affinity (pKd): 6.45
In this family, the difference between the best and least good affinity is small. This is because the sidechain contributing to binding is shared between both molecules. A covalent bond in molecule 193 may contribute to better binding affinity.		
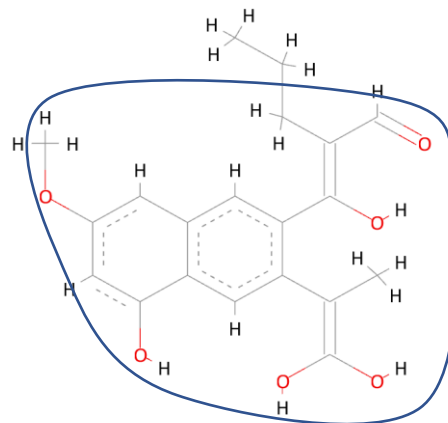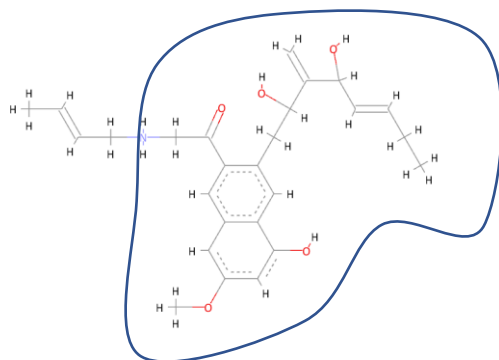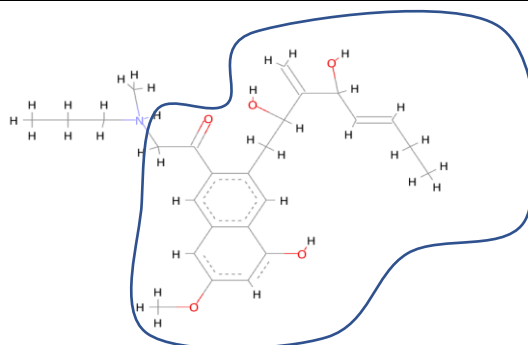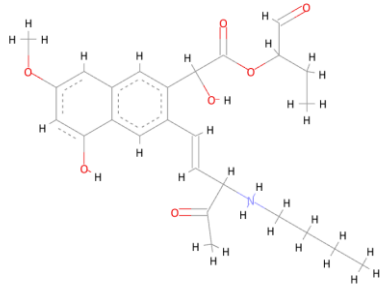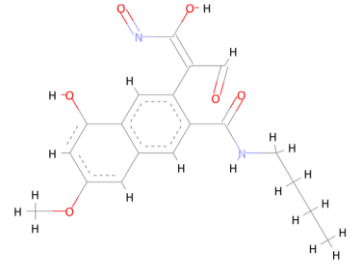
7	Molecule 194 Affinity (pKd): 6.56	Only one molecule was left in this family after filtering for Lipinski Rule Compliance.
A comparison could not be made as there was only one molecule was left after filtering for Lipinski Rule Compliance.		
8	Molecule 200 Affinity (pKd): 5.59	Only one molecule was left in this family after filtering for Lipinski Rule Compliance.
A comparison could not be made as there was only one molecule was left after filtering for Lipinski Rule Compliance.		

Table 4.2 comparing the structure of the highest and lowest affinity molecules from each family derived

from seed 25.2D molecules were rendered using BIOVA Discovery Studio Visualiser®.[6]

---

[6] Dassault Systèmes. BIOVIA Discovery Studio Visualizer. Version 20.1 [software]. Dassault Systèmes. 2020 [cited 2021 Jul 14; downloaded 2021 May 25]. Available from:
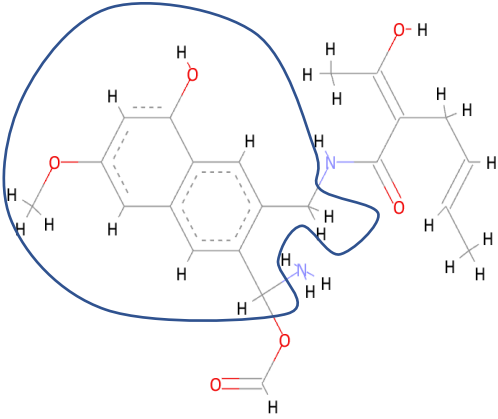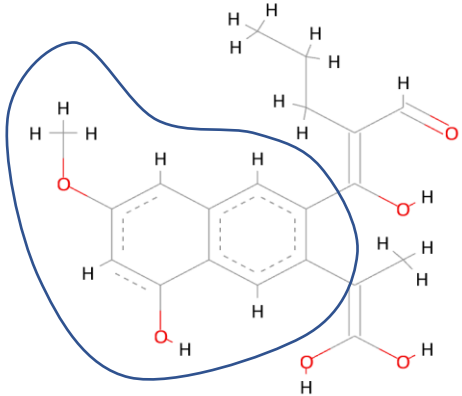
Optimally Binding	Molecular Structure Exhibiting the Lowest Affinity
Molecule 2 Family 2 Affinity (p*K*d): 8.3	Molecule 192 Family 5 Affinity (p*K*d): 5.45
A difference between both molecules can be seen in the amount of sidechain complexity. Molecule 2 contains 2 nitrogen atoms as part of an amino group which act as strong H-bond acceptors.	

Table 4.3 Comparing the structure of the best overall molecule and worst overall molecule derived from seed 1. 2D molecules were rendered using BIOVA Discovery Studio Visualiser®.[6]

---

https://www.3dsbiovia.com/products/collaborative-science/biovia-discovery-studio/visualization-download.php.

[6] Dassault Systèmes. BIOVIA Discovery Studio Visualizer. Version 20.1 [software]. Dassault Systèmes. 2020 [cited 2021 Jul 14; downloaded 2021 May 25]. Available from: https://www.3dsbiovia.com/products/collaborative-science/biovia-discovery-studio/visualization-download.php.
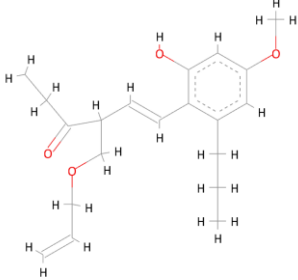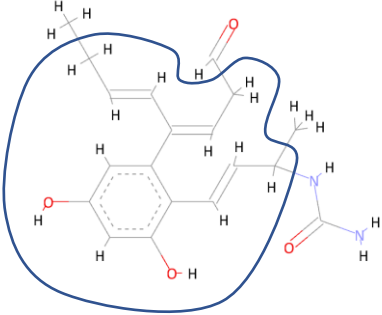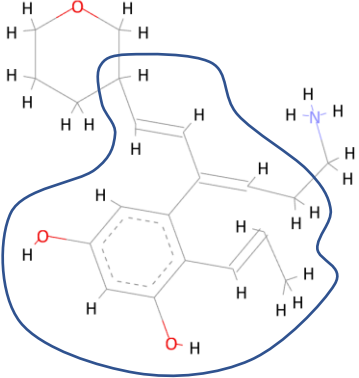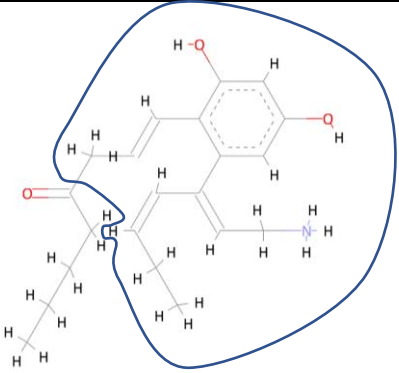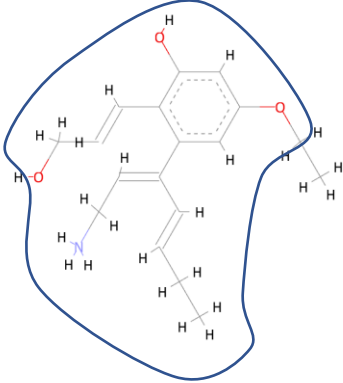
Family	Optimally Binding	Molecular Structure Exhibiting the Lowest Affinity
5	Molecule 010 Affinity (pKd): 5.03	Only one molecule was left in this family after filtering for Lipinski Rule Compliance.
A comparison could not be made as there was only one molecule was left after filtering for Lipinski Rule Compliance.		

Table 4.4 A comparison could not be made as there was only one molecule was left after filtering for Lipinski Rule Compliance. 2D molecules were rendered using BIOVA Discovery Studio Visualiser®.[6]

[6] Dassault Systèmes. BIOVIA Discovery Studio Visualizer. Version 20.1 [software]. Dassault Systèmes. 2020 [cited 2021 Jul 14; downloaded 2021 May 25]. Available from: https://www.3dsbiovia.com/products/collaborative-science/biovia-discovery-studio/visualization-download.php.

Family	Optimally Binding	Molecular Structure Exhibiting the Lowest Affinity
1	Molecule 001 Affinity (pKd): 7.96	Molecule 081 Affinity (pKd): 6.03
Molecule 1 has an amide with an amine group as compared to molecule 81 which has pyran ring.		
2	Molecule 083 Affinity (pKd): 7.52	Molecule 100 Affinity (pKd):6.04

Molecule 83 was more robust and has a longer chain than Molecule 100	
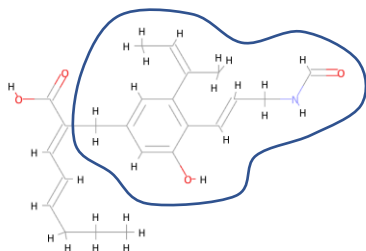
3	 Molecule 101 Affinity (pKd): 7.54	 Molecule 123 Affinity (pKd): 6.26
Molecule 101 contains a longer chain which includes a carboxyl group whilst molecule 123 contains an amide group and a cyclopentane ring.		
4	 Molecule 125 Affinity (pKd):7.21	 Molecule 143 Affinity (pKd): 6.03
Molecule 125 contains an amine group attached to a longer chain compared to the short hydroxyl group on molecule 143.		
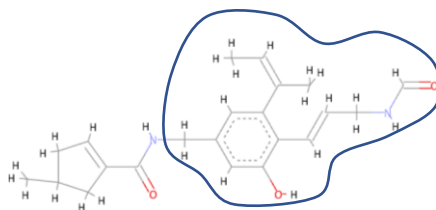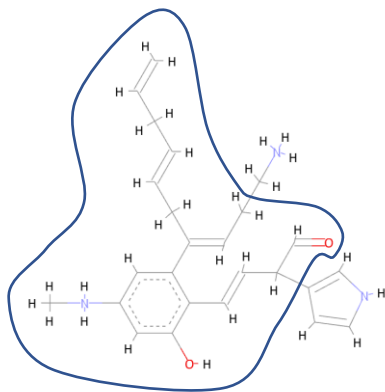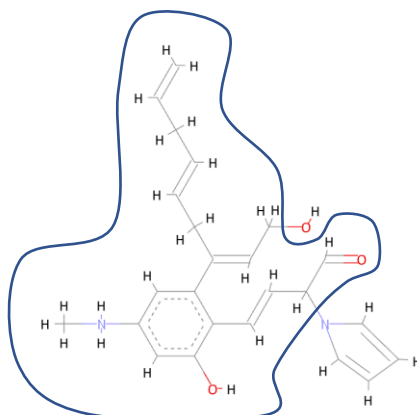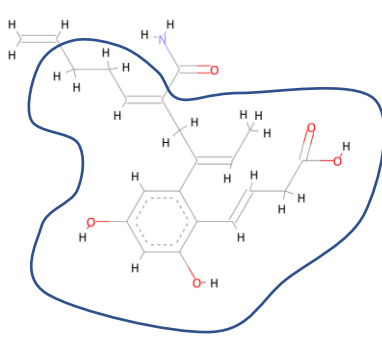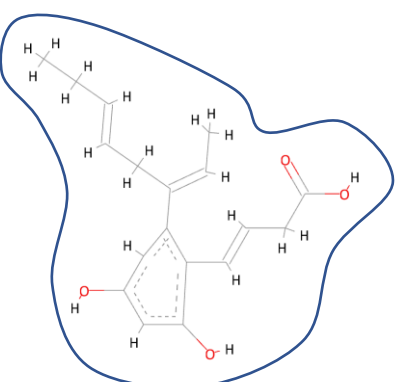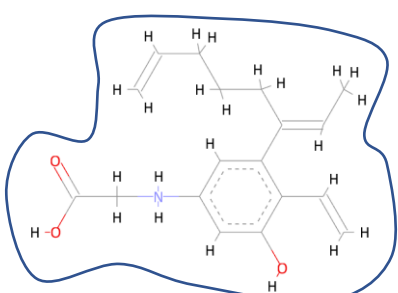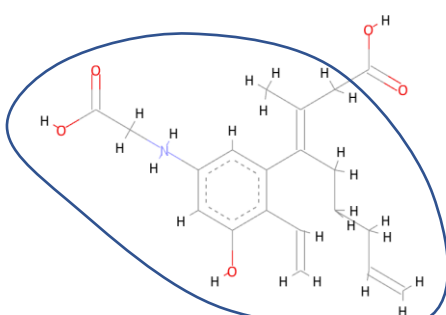
5	Molecule 144 Affinity (p*K*d): 7.05	Molecule 146 Affinity (p*K*d): 6.23

Molecule 144 is more robust than molecule 146 occupying the ligand binding pocket better.

6	Molecule 147 Affinity (p*K*d): 6.82	Molecule 171 Affinity (p*K*d): 6.07

In this family, the difference between the best and least good affinity is small.
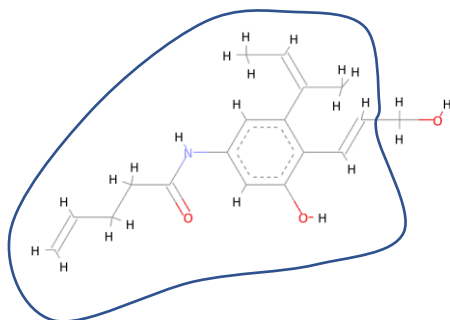
7	Molecule 173 Affinity (pKd): 6.31	Molecule 175 Affinity (pKd): 6.05
In this family, the difference between the best and least good affinity is small.		
8	Molecule 176 Affinity (pKd): 6.71	Molecule 179 Affinity (pKd): 6.37
In this family, the difference between the best and least good affinity is small.		
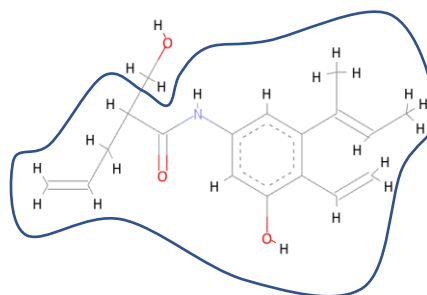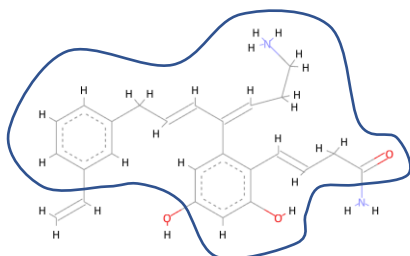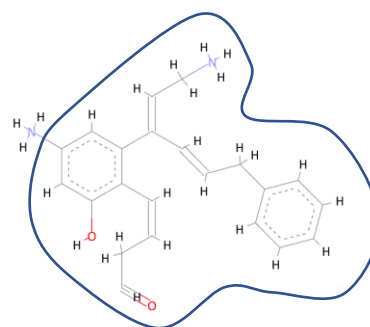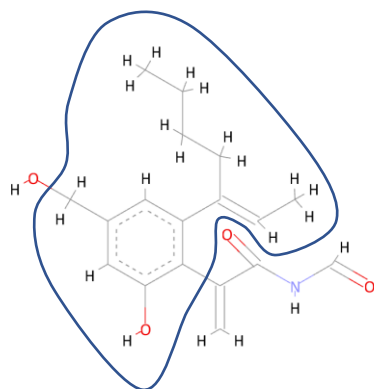
9	 Molecule 181 Affinity (pKd): 6.71	 Molecule 188 Affinity (pKd): 6.17
In this family, the difference between the best and least good affinity is small.		
10	 Molecule 189 Affinity (pKd): 6.64	 Molecule 195 Affinity (pKd): 6.07
In this family, the difference between the best and least good affinity is small.		
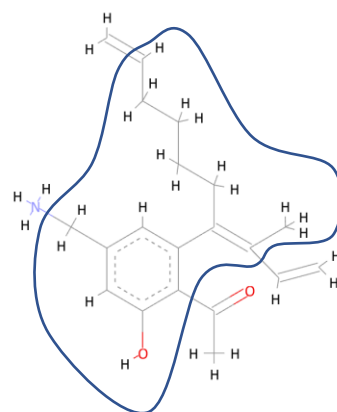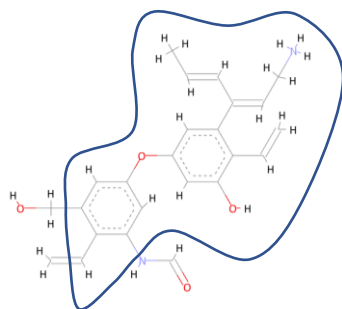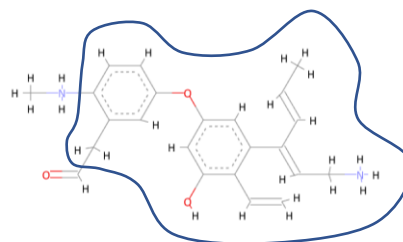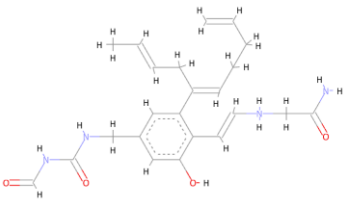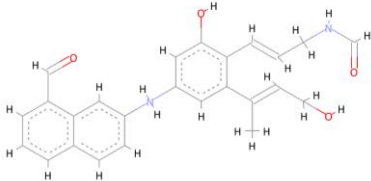
| 11	 Molecule 196 Affinity (p*K*d): 6.62	Only one molecule was left in this family after filtering for Lipinski Rule Compliance.
A comparison could not be made as there was only one molecule was left after filtering for Lipinski Rule Compliance.		
12	 Molecule 199 Affinity (p*K*d): 6.1	Only one molecule was left in this family after filtering for Lipinski Rule Compliance.
A comparison could not be made as there was only one molecule was left after filtering for Lipinski Rule Compliance.		
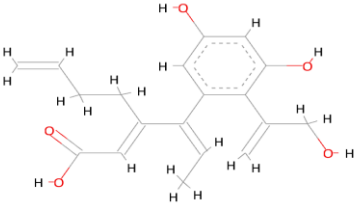
13	Molecule 200 Affinity (pKd): 6.45	Only one molecule was left in this family after filtering for Lipinski Rule Compliance.
A comparison could not be made as there was only one molecule was left after filtering for Lipinski Rule Compliance.		

Table 4.5 comparing the structure of the best and worst molecule from each family derived from seed 3.

2D molecules were rendered using BIOVA Discovery Studio Visualiser®.[6]

---

[6] Dassault Systèmes. BIOVIA Discovery Studio Visualizer. Version 20.1 [software]. Dassault Systèmes. 2020 [cited 2021 Jul 14; downloaded 2021 May 25]. Available from: https://www.3dsbiovia.com/products/collaborative-science/biovia-discovery-studio/visualization-download.php.

Optimally Binding	Molecular Structure Exhibiting the Lowest Affinity
Molecule 001 Family 1 Affinity (pKd): 7.96	Molecule 143 Family 5 Affinity (pKd): 5.45
Molecule 001 has a shorter sidechain however has an amide group which is bonded to a tertiary amine.	

Table 4.6 Comparing the structure of the best overall molecule and worst overall molecule derived from seed 1. 2D molecules were rendered using BIOVA Discovery Studio Visualiser®.[6]

[6] Dassault Systèmes. BIOVIA Discovery Studio Visualizer. Version 20.1 [software]. Dassault Systèmes. 2020 [cited 2021 Jul 14; downloaded 2021 May 25]. Available from: https://www.3dsbiovia.com/products/collaborative-science/biovia-discovery-studio/visualization-download.php.

A 2D topology map was created using the molecule with the highest affinity from both seed 1 and 3 obtained through the *de novo* process and the *apo* L*l*6PGD enzyme as shown in the image below.
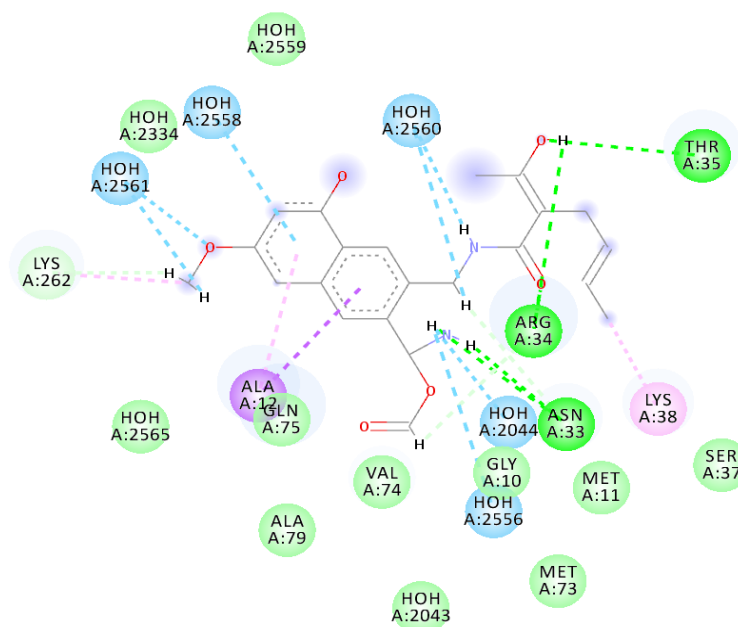
Figure 4.1 2D topology map of molecule with the highest affinity (molecule 6) of seed 1 obtained by the *de novo* process and the *apo* L*l*6PGD ligand binding pocket. Created in BIOVA Discovery Studio Visualiser®.[6]

[6] Dassault Systèmes. BIOVIA Discovery Studio Visualizer. Version 20.1 [software]. Dassault Systèmes. 2020 [cited 2021 Jul 14; downloaded 2021 May 25]. Available from: https://www.3dsbiovia.com/products/collaborative-science/biovia-discovery-studio/visualization-download.php.
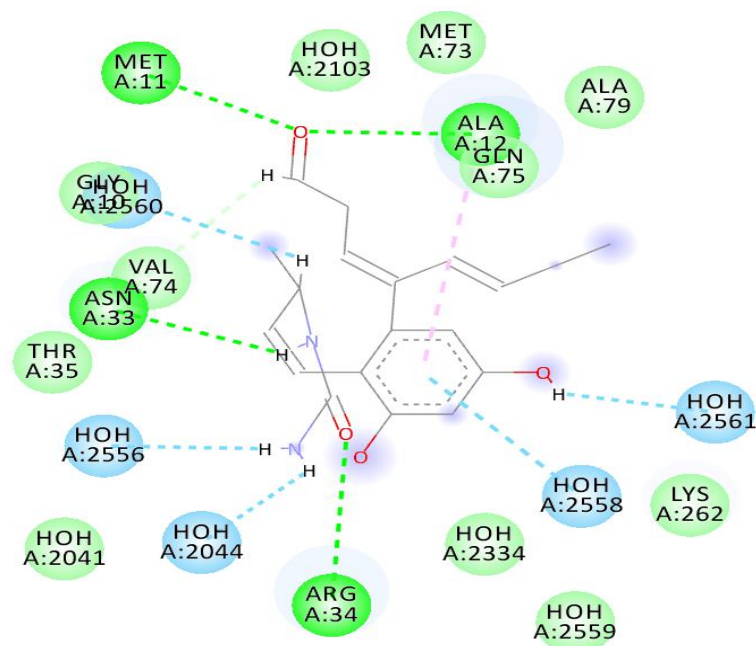
Figure 4.2 2D topology map of molecule with the highest affinity (molecule 1) of seed 3 obtained by the *de novo* process and the *apo* L*l*6PGD enzyme's ligand binding pocket. Created in BIOVA Discovery Studio Visualiser®.[6]

It is clearly shown that the highest-ranking molecule from the *de novo* exercise produced more robust interactions within the L*l*6PGD enzyme's ligand binding pocket compared to parietin. The amino acids implicated suggest that parietin shares the binding site with the co-factor NADP+ (Figure 4.3). In this case, Ala[12] is able to bind to parietin and even more to molecule 006 than the cofactor NADP+ as the latter co-factor is blocked due to the protrusion of the Ala[12] residue. Furthermore, molecule 006 forges more interactions with residues commonly shared with NADP+ such as Asn[33] which is considered crucial to NADP+ , Ala[12], Arg[34] and Thr[35] (Tetaud et al., 1999). Lin *et al*., (2015) suggested different

---

binding modalities than those observed in this study, however such variances may have been attributed to the different crystallographic depositions used (2iZ1 vs 3FWN), different binding site positions and the different protein-ligand interaction algorithms used. The highest-ranking molecule from seed 3 exhibits different binding modalities than those observed in parietin and molecule 6 of seed 1.
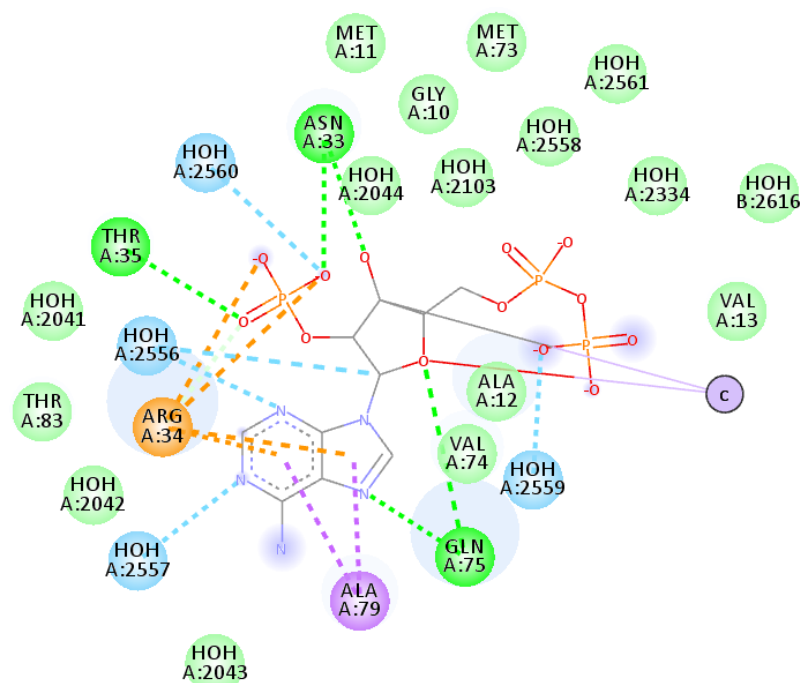
Image 4.3 2D topology map of NADP+ inside the *pdb* crystallographic deposition 2IZ1. Created in BIOVA Discovery Studio Visualiser®.[6]

[6] Dassault Systèmes. BIOVIA Discovery Studio Visualizer. Version 20.1 [software]. Dassault Systèmes. 2020 [cited 2021 Jul 14; downloaded 2021 May 25]. Available from: https://www.3dsbiovia.com/products/collaborative-science/biovia-discovery-studio/visualization-download.php.

The best 5 molecules from the *de novo* approach were also studied for their interaction with the L*l*6PGD enzyme's ligand binding pocket. The frequency of amino acids which took part in the interaction process were noted in Graph 4.1. It has been noticed that Ala[12], Arg[34] and Asn[33] and to a lesser extent Val[74] contribute to molecular binding within the L*l*6PGD ligand binding pocket. Interaction with these residues must consequently be considered important in the design of 6PGD modulators.
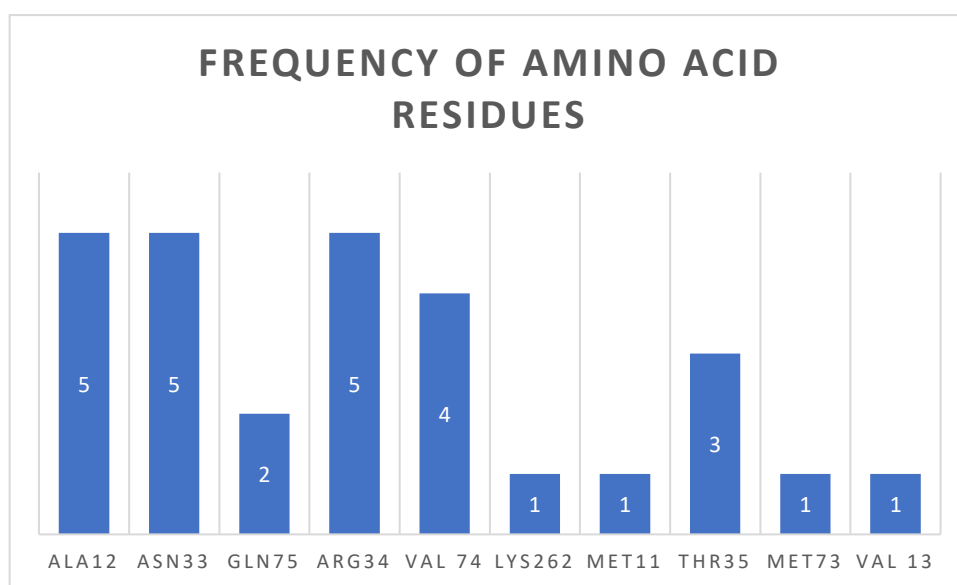
Figure 4.4 A graph showing the frequency of amino acid residues of the L*l*6PGD enzyme's ligand binding pocket that contributed to binding of the top 5 *de novo* molecules.

Limitations of the *de novo* process arises from the fact that molecular growth was based on a static L*l*6PGD ligand binding pocket. In reality, a protein is flexible and will change conformation to occupy and bind its ligand. As a result, with all *in silico* processes, the exact binding of a ligand with the protein cannot be exactly replicated.

Conclusion

This study explored the structurally diverse parietin scaffold as an alternative to that of the cognate small molecule inhibitor PEX to identify structures capable of 6PGD modulation. 4 Lipinski Rule compliant (Lipinski et al, 2001) hit molecules were identified using virtual screening and a series of molecules that occupied the 6PGD ligand binding pocket were generated with the *de novo* approach. The fact that these molecules interact with the 6PGD receptor with an LBA comparable to that of the cognate PEX small molecule inhibitor is particularly interesting from a drug design perspective.

References

Adams MJ, Archibald IG, Bugg CE, Carne A, Gover, S, Helliwell JR *et al*. The three dimensional structure of sheep liver 6-phosphogluconate dehydrogenase at 2.6 A resolution. EMBO J. 1983; 2(6): 1009-1014.

Adams MJ, Ellis GH, Gover S, Naylor CE, Phillips C. Crystallographic study of coenzyme, coenzyme analogue and substrate binding in 6-phosphogluconate dehydrogenase: implications for NADP specificity and the enzyme mechanism. Structure. 1994; 2(7): 651-668.

Ash S, Cline MA, Homer RW, Hurst T, Smith GB. ChemInform Abstract: Sybyl ® Line Notation (SLN): A versatile Language for Chemical Structure Representation. ChemInform. 2010;28(18):66-78.

Bačkorová M, Bačkor M, Mikeš J, Jendželovský R, Fedoročko P. Variable responses of different human cancer cells to the lichen compounds parietin, atranorin, usnic acid and gyrophoric acid. Toxicol In Vitro. 2011; 25(1): 37-44.

Basile A, Rigano D, Loppi S, Di Santi A, Nebioso A, Sorbo S *et al*., Antiproliferative, antibacterial and antifungal activity of the lichen Xanthoria parietina and its secondary metabolite parietin. Int J Mol Sci. 2015; 16(4): 7861-7875.

Bray F, Ferlay J, Soerjomatram I, Siegel RL., Torre LA., Jermal A. Global cancer statistics 2018: GLOBOCAN estimates of incidence and mortality worldwide for 36 cancers in 185 countries. CA Cancer J Clin. 2018; 68(6): 394-424

Cairns RA, Harris IS, Mak TW. Regulation of cancer cell metabolism. Nat Rev Cancer. 2011; 11(2): 85-95.

Chen X, Gao H, Han Y, Ye J, Xie J, Wang C. Physcion induces mitochondria-driven apoptosis in colorectal cancer cells via downregulating EMMPRIN. Eur J Pharmacol. 2015; 764: 124-133.

Chen H, Wu D, Bao L, Yin T, Lei D, Yu J, Tong X. 6PGD inhibition sensitizes hepatocellular carcinoma to chemotherapy via AMPK activation and metabolic reprogramming. Biomed Pharmacother. 2019; 111: 1353-1358

Elf S, Lin R, Xia S, Pan Y, Shan C, Wu S *et al.* Targeting 6-phosphogluconate dehydrogenase in the oxidative PPP sensitizes leukemia cells to antimalarial agent dihydroartemisinin. Oncogene. 2017; 36(2): 254-262.

Frisch SM, Francis H. Disruption of epithelial cell-matrix interactions induces apoptosis. J Cell Biol. 1994; 124(4): 619-626.

Gu J, Cui C, Yang L, Wang L, Jiang X. Emodin Inhibits Colon Cancer Cell Invasion and Migration by Suppressing Epithelial–Mesenchymal Transition via the Wnt/β-Catenin Pathway. Oncology Research. 2019; 27(2): 193-202

Guo H, Xiang Z, Zhang Y, Sun D. Inhibiting 6-phosphogluconate dehydrogenase enhances chemotherapy efficacy in cervical cancer via AMPK-independent inhibition of RhoA and Rac1. Clinical and Translational Oncology. 2018; 21(4): 404-411

Hanau S, Montin K, Cervellati C, Magnani M, Dallocchio F. 6-Phosphogluconate Dehydrogenase Mechanism: Evidence for allosteric modulation by substrate. J Biol Chem. 2010; 285(28): 21366-21371.

Hilbig M., Rarey M. MONA 2: a light cheminformatics platform for interactive compound library processing. J. Chem. Inf. Model. 2015; 55(10): 2071–2078.

Johnson WJ, Mccoll JD. 6-Aminonicotinamide—a Potent Nicotinamide Antagonist. Science. 1995; 122(3174): 834.

Koes DR, Camacho CJ. ZINCPharmer: pharmacophore search of the ZINC database. Nucleic Acids Res. 2012; 40(W1): W409-W414.

Lange K, Proft ER. Inhibition of the 6-phosphogluconate dehydrogenase in the rat kidney by 6-aminonicotinamide. Naunyn Schmiedebergs Arch Pharmacol. 1970; 267(2): 177-180.

Lehninger AL, Nelson DL, Cox MM. Lehninger Principles of Biochemistry. 4th ed. New York: W.H. Freeman; 2005. p. 549-555.

Li Y, Luan Y, Qu X, Li M, Gong L, Xue X *et al.* Emodin Triggers DNA Double-Strand Breaks by Stabilizing Topoisomerase II-DNA Cleavage Complexes and by Inhibiting ATP Hydrolysis of Topoisomerase II. Toxicol Sci. 2010; 118(2): 435-443.

Li C, Ma J, Zheng L, Li H, Li P. Determination of emodin in L-02 cells and cell culture media with liquid chromatography–mass spectrometry: Application to a cellular toxicokinetic study. J PHARM BIOMED ANAL. 2012; 71: 71-78.

Lin CJ, Elf S, Shan C, Kang H, Ji Q, Zhou Lu. 6-Phosphogluconate dehydrogenase links oxidative PPP, lipogenesis and tumour growth by inhibiting LKB1–AMPK signalling. Nat Cell Biol. 2015; 17(11): 1484-1496.

Lipinski CA, Lombardo F, Dominy BW, Feeney Pj. Experimental and computational

approaches to estimate solubility and permeability in drug discovery and development settings. Advanced Drug Delivery Reviews 2015; 46(1-3):3-26.

Liu W, He J, Yang Y, Guo Q, Gao F. Upregulating miR-146a by physcion reverses multidrug resistance in human chronic myelogenous leukemia K562/ADM cells. Am. J. Cancer Res. 2016; 6(11): 2547-2560.

Mandal S, Moudgil M, Mandal SK. Rational drug design. Eur J Pharmacol. 2009; 625(1-3): 90-100.

Pan X, Wang C, Li Y, Huang L. Physcion induces apoptosis through triggering endoplasmic reticulum stress in hepatocellular carcinoma. Biomed Pharmacother. 2018a; 99: 894-903.

Pan X, Wang C, Li Y, Zhu L, Zhang T. Protective autophagy induced by physcion suppresses hepatocellular carcinoma cell metastasis by inactivating the JAK2/STAT3Axis. Life Sciences. 2018b; 214: 124-135.

Pandolf PP, Sonati F, Rivi R, Mason P, Grosveld F, Luzzato L. Targeted disruption of the housekeeping gene encoding glucose 6-phosphate dehydrogenase (G6PD): G6PD is dispensable for pentose synthesis but essential for defense against oxidative stress. EMBO J. 1995; 14(21): 5209-5215.

Petterson EF, Goddard TD, Huang CC, Couch GS, Greenblatt DM, Meng E *et al*. UCSF Chimera--a visualization system for exploratory research and analysis. J Comput Chem. 2004; 25(13): 1605-1612.

Qin X, Peng Y, Zheng J. In Vitro and in Vivo Studies of the Electrophilicity of Physcion and its Oxidative Metabolites. Chem. Res. Toxicol. 2018; 31(5): 340-349.

Richardson AD, Yang C, Osterman A, Smith JW. Central carbon metabolism in the progression of mammary carcinoma. Breast Cancer Res Treat. 2008; 110(2): 297-307.

Schafer ZT, Grassian AR, Song L, Jiang Z, Gerhart-Hines Z, Irea HY. Antioxidant and oncogene rescue of metabolic defects caused by loss of matrix attachment. 2009; 461(7260): 109-113.

Shan C, Elf S, Ji Q, Kang H, Zhou L, Hitosugi T. Lysine Acetylation Activates 6-Phosphogluconate Dehydrogenase to Promote Tumor Growth. Molecular Cell. 2014; 55(4): 552-565.

Silverberg M, Dalziel K. Crystalline 6-Phosphoglconate Dehydrogenase from Sheep Liver. Eur J Biochem. 1973; 38: 229-238.

Sundaramoorthy R, lulek J, Barret MP, Bidet O, Ruda GF, Gilbert IH *et al.* Crystal structures of a bacterial 6-phosphogluconate dehydrogenase reveal aspects of specificity, mechanism and mode of inhibition by analogues of high-energy reaction intermediates. FEBS J. 2007; 274(1): 275-276.

Tetaud E, Hanau S, Wells JM, Le Page RW, Adams MJ, Arkinson S *et al.* 6-Phosphogluconate dehydrogenase from Lactococcus lactis: a role for arginine residues in binding substrate and coenzyme. Biochem J. 1999; 338(1): 55-60.

Tsang-Bin T, Wei-Kuo C, Tien-Yu H, Pei-Tzu W, Wen-Chuan H, Catherine L et al. Safety and Tolerability of Physcion in Healthy Volunteers in a Phase I Dose Escalating Clinical Pharmacology Study. Gastroenterology. 2011; 140(5): S-572.

Wang R, Gao Y, Lai L. Ligbuilder: A multi-purpose program for structure-based drug design. Journal of Molecular Modeling 2000; 6(7-8): 498-516

Wang R, Lai L, Wang S. Further development and validation of empirical scoring functions for structure-based binding affinity prediction. J Comput Aided Mol Design. 2002; 16(1): 11-26.

Wood T. Physiological functions of the pentose phosphate pathway. Cell Biochem Funct. 1986; 4(4): 241-247.

Yan-Tao H, Xue-Hong C, Hui G, Jun-Li Y, Chun-Bo W. Physcion inhibits the metastatic potential of human colorectal cancer SW620 cells in vitro by suppressing the transcription factor SOX2. Acta Pharmacol Sin. 2015; 37(2): 264-275.

List of Publications and Abstracts

L-Università ta' Malta

Daniel Sinagra <daniel.sinagra.16@um.edu.mt>

CMC Submission Acknowledgement | BMS-CMC-2021-484

Current Medicinal Chemistry <admin@bentham.manuscriptpoint.com>   28 August 2021 at 15:10
Reply-To: Current Medicinal Chemistry <cmc@benthamscience.net>
To: daniel.sinagra.16@um.edu.mt
Cc: cmc@benthamscience.net

Reference#: BMS-CMC-2021-484

Submission Title: Rational Design and Preliminary Validation of Novel 6-Phosphogluconate Dehydrogenase (6PGD) Inhibitors Using Parietin as a Lead

Dear Dr. Daniel Sinagra,

Thank you for submitting your abstract to "Current Medicinal Chemistry".

Your abstract will be peer reviewed and you will be informed about the final editorial decision.

Sincerely,

Editorial Office
Current Medicinal Chemistry
Bentham Science Publishers

To unsubscribe from MPS and stop receiving emails further. Please send an email to unsubscribe@bentham.manuscriptpoint.com.

Powered by Bentham Manuscript Processing System

L-Università ta' Malta

Daniel Sinagra <daniel.sinagra.16@um.edu.mt>

Sciforum.net submission received [sciforum-049986]

info@sciforum.net <info@sciforum.net>   28 August 2021 at 15:22
Reply-To: ecmc@mdpi.com
To: daniel.sinagra.16@um.edu.mt
Cc: daniel.sinagra.16@um.edu.mt, drclaireshoemake@gmail.com

Dear Daniel Sinagra,

Thank you for sending us your abstract. It will be evaluated by the Scientific Committee and you will be notified about acceptance by 21st October 2021. If revisions are necessary, you will be contacted prior to that date.

Submission ID: sciforum-049986
Title: Rational Design and Preliminary Validation of Novel 6-Phosphogluconate Dehydrogenase (6PGD) Inhibitors Using Parietin as a Lead
Authors: Daniel Sinagra *, Claire Shoemake
Event: 7th International Electronic Conference on Medicinal Chemistry
Section: General

Comments: Research paper as part of my dissertation of the Master in Pharmacy postgraduate studies at the University of Malta

https://sciforum.net/dashboard/author/submissions/655b2693245ddc61b02b7f4bae130602

Kind regards,
Your ECMC2021 Organizing Team
ecmc@mdpi.com

Sciforum.net is a platform published and maintained by MDPI.
For technical support, email info@sciforum.net
Facebook Twitter

L-Università
ta' Malta

Daniel Sinagra <daniel.sinagra.16@um.edu.mt>

Sciforum.net abstract approved [sciforum-049986]

info@sciforum.net <info@sciforum.net>   28 August 2021 at 17:44
Reply-To: ecmc@mdpi.com
To: daniel.sinagra.16@um.edu.mt
Cc: daniel.sinagra.16@um.edu.mt, drclaireshoemake@gmail.com

Dear Daniel Sinagra,

We are pleased to inform you that your abstract has been approved by our editorial team.

Please make sure to upload your submission files before the full submission deadline. You can access your submission through the link below:

The editors have made some changes to the submission title and/or abstract fields: please double check the changed values (you can see the original versions in the submission view history).

Submission ID: sciforum-049986
Title: Rational design and preliminary validation of novel 6-phosphogluconate dehydrogenase (6PGD) inhibitors using parietin as a lead
Authors: Daniel Sinagra *, Claire Shoemake
Event: 7th International Electronic Conference on Medicinal Chemistry
Section: General

Editor decision: Approve
Editor comments: Dear Colleagues, Many thanks for your confidence and your submission. The abstract will appear immediately online. Feel free to upload your work at your best convenience. You have choice between four panels: poster, slideshow, flash communication (5 min), or communication (15-30 min). We shall direct your contribution to the appropriate panel after acceptation. Please use the template provided on the website of the conference and strictly follow the instructions for authors. Be sure that the text of the poster/slides will be checked by a native English-speaking scientist. Additional round tables could be created depending on the number of submissions we receive. If you have any question, feel free to contact me. Many thanks for disseminating the event. Stay safe Best regards JJ Vanden Eynde Chairman

https://sciforum.net/dashboard/author/submissions/655b2693245ddc61b02b7f4bae130602

Kind regards,
Your ECMC2021 Organizing Team
ecmc@mdpi.com

Sciforum.net is a platform published and maintained by MDPI.
For technical support, email info@sciforum.net
Facebook Twitter

Appendix 1: Ethics Approval Email

L-Università ta' Malta

Daniel Sinagra <daniel.sinagra.16@um.edu.mt>

FRECMDS_2021_181 - ID:- 9558_06091998_Daniel Sinagra

5 messages

FACULTY RESEARCH ETHICS COMMITTEE <research-ethics.ms@um.edu.mt>   27 August 2021 at 10:10
To: Daniel Sinagra <daniel.sinagra.16@um.edu.mt>
Cc: "Dr. Claire Shoemake" <drclaireshoemake@gmail.com>

Dear Mr Sinagra,

Good morning and thank you for submitting your application, however you still have some documents missing that you need to submit, in order to continue with your research.

Kindly provide us with the following documents, as a reply to this email, please:

- CV of researcher/s
- Supervisor's endorsement (an email stating that she endorses this research would suffice)
- Protocol (detailed account of study)
- Proposal (overview of study)

Note: It is important to provide the Proposal and Protocol into two separate documents, since the Proposal is an overview of the study, whilst the Protocol is a detailed account of the study.

Thanks and regards,
Annalise

L-Università ta' Malta

Annalise Mallia Duca | Secretary

Faculty Research Ethics Committee
Faculty of Medicine and Surgery
Medical School, Mater Dei Hospital
+356 2340 1803

https://www.um.edu.mt/ms/students/researchethics

On Tue, 24 Aug 2021 at 21:16, Daniel Sinagra <daniel.sinagra.16@um.edu.mt> wrote:
Dear all,

Please find attached a copy of my FREC/ UREC form.

Kind regards,
Daniel.

Daniel Sinagra <daniel.sinagra.16@um.edu.mt>   27 August 2021 at 11:33
To: FACULTY RESEARCH ETHICS COMMITTEE <research-ethics.ms@um.edu.mt>

Dear Annalise,

Please find attached all relevant documents. Waiting on supervisor endorsement.

Kind Regards,
Daniel
[Quoted text hidden]

3 attachments

📄 Daniel_Sinagra_CV[682].pdf
34K

📄 **Protocol.pdf**
248K

📄 **Proposal.pdf**
3090K

Dr. Claire Shoemake <drclaireshoemake@gmail.com>   27 August 2021 at 13:34
To: FACULTY RESEARCH ETHICS COMMITTEE <research-ethics.ms@um.edu.mt>
Cc: Daniel Sinagra <daniel.sinagra.16@um.edu.mt>

I endorse Daniel Sinagra's study.

Best Regards,

Dr. C. Shoemake
[Quoted text hidden]

FACULTY RESEARCH ETHICS COMMITTEE <research-ethics.ms@um.edu.mt>   30 August 2021 at 11:53
To: Daniel Sinagra <daniel.sinagra.16@um.edu.mt>
Cc: Claire Shoemake <claire.zerafa@um.edu.mt>

Dear Mr Sinagra,

Since your self-assessment resulted in no issues being identified, FREC will file your application for record and audit purposes but will not review it.

Any ethical and legal issues including data protection issues are your responsibility and that of the supervisor.

Good luck with your project!

Regards,
Annalise
[Quoted text hidden]
[Quoted text hidden]

Daniel Sinagra <daniel.sinagra.16@um.edu.mt>   30 August 2021 at 18:25
Draft To: FACULTY RESEARCH ETHICS COMMITTEE <research-ethics.ms@um.edu.mt>

[Quoted text hidden]

Addendum

A CD containing all the relevant raw data used in this project. This includes;

- A Microsoft® Excel® file containing all molecules generated through Ligbuilder® v1.2

- Affinities calculated through x-Score® v1.2